Evaluation of the superselective radioligand [^{123}I]PE2I for imaging of the dopamine transporter in SPECT.

Morten Ziebell

This review has been accepted as a thesis together with four previously published papers by University of Copenhagen 20th of January 2011 and defended on 18th of March 2011.

Tutor: Gitte Moos Knudsen

Official opponents: Lars Friberg, Jan Booij, Anna M. Catafau.

Correspondence: Department of Neurology, Neurobiology Research Unit, Copenhagen University Hospital, Rigshospitalet, Blegdamsvej 9, 2100 Copenhagen. Denmark

E-mail: ziebell@nru.dk

Dan Med Bull 2011;58(5): B4279

THE 4 ORIGINAL PAPERS ARE

1. Pinborg LH, Ziebell M, Frokjaer VG, de Nijs R, Svarer C, Haugbol S, Yndgaard S, Knudsen GM (2005) Quantification of 123I-PE2I binding to dopamine transporter with SPECT after bolus and bolus/infusion. J Nucl Med 46:1119-27.

2. Ziebell M, Thomsen G, Knudsen GM, de Nijs R, Svarer C, Wagner A, Pinborg LH (2007) Reproducibility of [123I]PE2I binding to dopamine transporters with SPECT. Eur J Nucl Med Mol Imaging 34:101-9.

3. Ziebell M, Pinborg LH, Thomsen G, de Nijs R, Svarer C, Wagner A, Knudsen GM (2010) MRI-guided region-of-interest delineation is comparable to manual delineation in dopamine transporter SPECT quantification in patients: a reproducibility study. J Nucl Med Technol 38:61-8.

4. Ziebell M, Holm-Hansen S, Thomsen G, Wagner A, Jensen P, Pinborg LH, Knudsen GM (2010) Serotonin transporters in dopamine transporter imaging: A head-to-head comparison of dopamine transporter SPECT radioligands [123I]FP-CIT and [123I]PE2I. J Nucl Med 51:1885-91.

BACKGROUND

Dopamine

In 2000 a Swedish scientist, Arvid Carlsson, received the Nobel Prize for his work with 3,4-dihydroxyphenethylamine, dopamine (DA) [1]. DA was synthesised in 1910 by George Barger and colleagues [2]. They found it to be a weak sympathomimetic compound and so it was left unexplored for more than three decades. What Arvid Carlsson found out years later, was that dopamine was a neurotransmitter by itself and not only a precursor for norepinephrine and epinephrine. In the same period the enzyme aromatic-L-amino-acid decarboxylase (also called dopa decarboxylase or AAAD) was discovery by a German scientist [3]. The discovery of this enzyme, which in mammalian tissues converts 3,4-dihydroxyphenylalanine (L-DOPA) to dopamine, provided a mechanism for the formation of dopamine in the brain because unlike dopamine itself, L-DOPA can cross the blood brain barrier (BBB). Since then the neurotransmitter dopamine has been the subject of enormous scientific interest; mentioned in almost 65.000 papers when combined with search term “brain” in a Pubmed search in September 2010.
DA neurons play a key role in many basic functions of the brain, such as motivation, motor behaviour and working memory. It constitutes one of its main functions in the reward system of the brain and thereby indirectly controls the learning of many of our specific behaviours (for review [4]). Altogether DA acts as a central neurotransmitter for our good health – mentally as physically. The DA neurons are located in groups deep within the brain and the projections of the DA neurons were originally identified and localized using the Falck – Hillarp histoflourocense method [5]. The most prominent cell group of DA neurons that accounts for 90 % of the total amount is located in the mesencephalon. There are 3 overall pathways in this DA system, fig. 1: In two of the pathways DA neuron cell bodies located in the ventral tegmental area project to the frontal cortex and the nucleus accumbens. In the third pathway, “the nigrostriatal pathway” DA neurons in the substantia nigra pars compacta (SNpc) project axons to the dorsal striatum (putamen and caudate nucleus), as part of the basal ganglia. This nigrostriatal pathway was first described in 1964 [6] and will be the focus of this thesis.

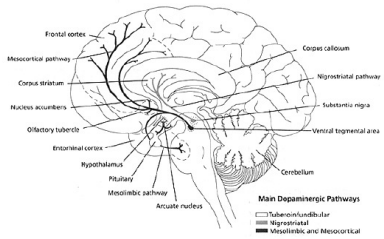

Figure 1. A sketch of the dopaminergic projections from the SNpc and the ventral tegmental area. (Source: *Aust Prescr* 1994; 17: 17-21).

The basal ganglia

The basal ganglia or basal nuclei are a group of nuclei situated in the forebrain (prosencephalon), fig. 2. The main components are the striatum, pallidum, substantia nigra and the subthalamic nucleus.

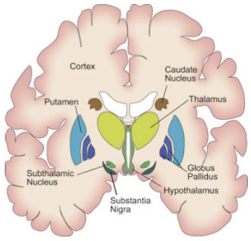

Figure 2. An overview of the different nuclei that make up the basal ganglia (thalamus, however not conventionally regarded as such). (Source: The Dana Foundation, unknown illustrator).

The striatum is mostly known for its part in planning and modulation of movement pathways, but it is also involved in different cognitive functions and in the reward system of the brain [4]. The striatum receives input not only from the SNpc but also from other brain areas such as the brain stem (raphe nucleus) that sends projections from serotonergic (5-HT) neurons [7]. However, the most dominant input comes from the neocortex, except the primary visual and auditory cortex, thus making striatum the major input center of the whole brain.

The striatum consists mostly of medium spiny neurons, which are inhibitory neurons that use γ-Aminobutyric acid (GABA) as neurotransmitter. The medium spiny neurons contain different types of neuropeptide receptors (Substance P, dynorphin and dopamine). Within the basal ganglia there is a very complex system of neuronal circuits. Two are major, fig. 3: "The direct pathway" where medium spiny neurons send their axons to the internal part of the globus pallidus and the substantia nigra, and "the indirect pathway" where they send their axons to the external part of the globus pallidus. In a complex pattern the net result of excitatory inputs towards medium spiny neurons in these two circuits either stimulates (the direct pathway) or inhibits (the indirect pathway) upper motor neurons and thereby movement.

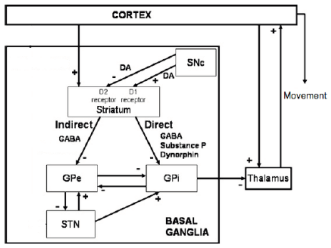

Figure 3. Scheme of the basal ganglia circuit. SNc Substantia nigra pars compacta; STN subthalamic nucleus; GPe & GPi external and internal part of the globus pallidus. (Source: Moroney, R, *Jour of Comput Neurosc* Vol. 25 Issue 3)

Not surprisingly dysfunction of the basal ganglia primarily leads to diseases associated with symptoms of movement dysfunction known as movement disorders such as Parkinson's disease (PD), Huntington's disease (HD), Lewy body dementia (DLB) and various other atypical Parkinson syndromes associated with basal ganglia pathology. These diseases involve different localisation in the basal ganglia. In HD there is a massive loss of medium spiny neurons in the striatum [8], whereas loss of neurons (i.e. dopaminergic neurons) is located in the SNpc in PD [9].

Dopamine transmission

The neurotransmission in the nigro-striatal pathway takes place in the dorsal striatum. DA is synthesized in the core of the DA neurons in SNpc and transported to the synapse where it is stored in presynaptic vesicles. When the DA neuron is triggered by electrical stimuli the DA is released into the synapse where it acts through DA receptors on the postsynaptic membrane. There are at least 5 receptors (D1-D5) belonging to the family of G-protein coupled transmembrane receptors [10]. D1 and D2 receptors are located in the striatum where they are involved in the direct and indirect motor loop [11].
Immediately after DA has carried out its action on the postsynaptic membrane it is removed from the synaptic cleft ensuring the effect of a new DA release at the next neurotransmission. Most of the extracellular DA is re-cycled by reuptake in the presynaptic cell by the dopamine transporter (DAT). Inside the cell, DA is either degraded by the monoamine oxidase (MAO) enzymes or vesicle-stored through the vesicular monoamine transporters (mainly type 2, VMAT2) [12]. This thesis has its main focus on in vivo imaging of the DAT as a surrogate marker for the DA neurotransmission to assign the state of function of the nigro-striatal pathway.

The dopamine transporter

The DAT, along with the serotonin and norepinephrine transporter (SERT and NET), are plasma membrane spanning proteins belonging to the SLC6 gene family transporters fig. 4, [13].

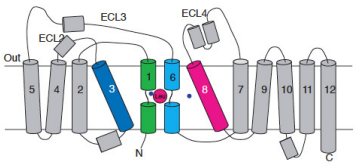

Figure 4. High-resolution structure of Na^+ - Cl^- -coupled neurotransmitter transporter homolog (SLC6 family). (Source Gether *et al* 2006).

The DAT constitutes of 620 amino acids residues [14] that actively clears extracellular dopamine, using the energy of cellular ionic electrochemical gradients [13]. DA uptake is dependent on the co-transport of Na+ and Cl-, and is driven by the ion concentration gradient facilitated by the Na+/K+ ATPase [14]. The DAT is a target of several clinically used drugs such as methylphenidate, d-amphetamine, and modafinil. In addition, the reinforcing and euphoric effects of the powerfully addictive stimulants cocaine and d-methamphetamine are primarily mediated by blocking the DAT leading to elevated extracellular DA concentration [15, 16]. DAT is expressed exclusively in DA neurons [17] and thus constitutes a specific marker of these neurons. Sub-localization is predominantly in axons and therefore high concentrations are observed in regions receiving DA afferents (striatum). However, DAT is not located in the synaptic zone but extrasynaptic, along the axons [18]. Recently the idea of the DA synapse has been

challenged and it has been proposed that DAT has its main role in the lifetime of extrasynaptic DA concentration more than a transporter for synaptic DA spillover, suggesting that DAT functions to regulate DA concentrations within a wide area rather than within the synaptic cleft fig. 5 [12, 16].

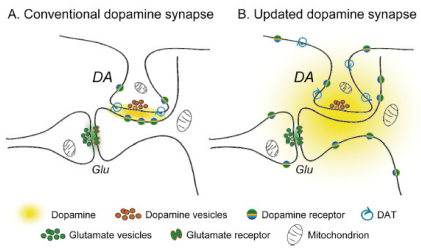

Fig. 5. Illustration of the conventional (A) and the updated (B) DA synapse (Source (Rice and Cragg 2008)).

The cell surface concentration of the DAT is dynamic and regulated primarily by membrane endocytosis [19] rather than de novo synthesis, which is relatively slow [20]. The rate of DAT cell surface up-/downregulation can be very rapid (seconds to minutes) and slow (days to weeks) which can be observed by the paradox effect on DAT expression after acute and long-term exposure to cocaine [21, 22]. In addition to drug induced regulation of the DAT, there are several proteins associated with regulation of the DAT, amongst those also some that play key roles in e.g. Parkinson's disease (for review [23]).

Parkinson's disease

PD was first described by James Parkinson [24] and is characterised by 4 core symptoms: rigidity, bradykinesia, tremor and postural instability. PD is the second most common neurodegenerative disorder after Alzheimer's disease with a 2005 prevalence of 1 % of people above 60 years [25]. Median age of onset of PD is 60 and average duration from diagnosis until death is 15 years [26]. However, late stages of PD involves severe disabilities with low quality of life and huge economic consequences for the society [27].

PD is considered a sporadic disease by which aging is the major risk factor, similar to other neurodegenerative disorders. Surprisingly, considering the substantial focus on the topic, very few environmental factors causing PD have been identified [28]. In recent years there has been focus on smoking and caffeine both known to cause release of dopamine in different nuclei in the basal ganglia [29, 30]. However, currently the proposed protective effect of these stimulants is somewhat controversial [31]. Genetic studies have shown involvement of genes in which mutations can lead to L-dopa responsive parkinsonism and in 10-15 % of patients with PD there is a positive family history compatible with a Mendelian inheritance [32].

The pathological hallmark of PD is the regional loss of DA cells in the SNpc that correlates to duration of disease [9]. The loss of DA neurons in PD is more precisely an increased acceleration in striatal neurodegeneration estimated to ~ 46 % per decade compared to the normal age-related loss of 6 % [33-35].

Involvement of the 5-HT system in PD is more unresolved. A post mortem brain study showed a marked decrease in many different markers of the 5-HT system, only the SERT binding showed a wide overlap with the normal controls [36] and this preservation in the early PD patients has recently been confirmed in a PET study [37]. Data have shown that there could be a "reactive" hyper-innervation of 5-HT neurons accompanying the DA neurodegeneration [38] and that this innervation plays an important role in L-DOPA induced dyskinesias experienced by some of the patients when treated [39]. Other midbrain areas may also be involved in PD although these mostly do not correlate to disease duration and hence their relation to the neurodegeneration in PD are disputed [9].

Diagnosis of PD

There are many clinical differential diagnoses to PD and especially in the beginning when symptoms are weak and history is short it can be difficult to diagnose the disease. In one study the concordance between an initial clinical diagnosis and a final diagnose settled by autopsy (>10 years later) showed a sensitivity of 75%, and a specificity of 42% [40]. However, as a consequence of the natural clinical progression of PD and other related diseases with striatal neurodegeneration, one can increase the clinical predictive values by following the patients since their symptoms will definitely persist and often worsen over time [41]. Clinicopathological studies suggest that when established PD is diagnosed according to current U.K. Brain Bank criteria, which is only possible when the PD patients have had symptoms for many years, there is a more than 80% concordance between expert clinical impression and the presence of nigral Lewy bodies [42].

Treatment of PD

Even though rasagiline vs. placebo in a large double-blind delayed-start trial seemed to slow the clinical progression of PD [43], the cure for PD remains unfound and symptomatic treatment is the only opportunity.

Biomarkers in PD

For PD and other related striatal neurodegenerative diseases the need for biomarkers in support of a clinical diagnosis or to assess progression of the disease in, e.g., intervention studies has long been a subject of intense investigation. Explored biomarkers in the cerebrospinal fluid include α-synuclein, tau protein and amyloid beta measurements but as of today most published reports have identify cerebrospinal fluid biochemistry as a useless diagnostic tool [44].

Despite the cell loss in SNpc, conventional MRI shows normal SNpc structure in patients with PD and is therefore not diagnostically helpful [45]. Newer methods such as Inversion recovery sequences [46] and T2-weighted sequences [47] are promising techniques, but even these MR images show a considerable overlap between PD and healthy controls. Newer 3 Tesla volumetric T1-weighted MRI studies have shown slight atrophy of the putamen compared to normal age matched controls, but failed to detect a reduction in SNpc volume in patients with PD, possibly because of difficulties in accurately defining the border of the SNpc [48]. So far the most promising results have been achieved by diffusion tensor imaging, where a recent study was able to differentiate 14 healthy subjects from 14 PD patients, because all the patients with PD showed a reduced Nigral fractional anisotropy [49]. These results should be replicated and evaluated in larger populations of PD patients.

METHODS

SPECT imaging

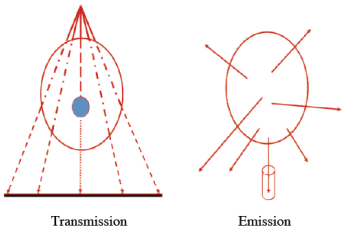

Figure 6. Illustration of the difference between a normal x-ray (to the left) that uses an external source that emits gamma ray's (transmission) and SPECT/PET where injection of radiotracer converts the subject into the radioactive source emitting gamma ray's (emission).

Single Photon Emission Computer Tomography (SPECT) began early after the introduction of computer science in the 1960s [50]. Some of the pioneer work in SPECT brain imaging actually took place in Copenhagen [51]. The method is a non-invasive technique that allows scientists to study various physiological and pathophysiological human brain functions in vivo. The basic technique requires injection of a molecule labelled with a radioactive gamma-emitting radioisotope (radionuclide) into the bloodstream of the patient. SPECT imaging is based on the injection of tracer amounts of the labelled molecule (nano- to picomoles, ie, much lower than the mili- to micromolar levels that elicit a pharmacologic response). The radioactive decay results in emission of photons (fig. 6) and these gamma ray's carry information of the location of the decay e.g. in the brain and thus the biodistribution of the radiotracer. Usually the half-life of the isotopes is much higher in SPECT than in Photon Emission Tomografy (PET) and thereby allows for transportation of the radioligand outside production facilities, lowering the costs and making the clinical application easier. As a downside the emission of only one gamma ray in SPECT, opposite the consequently two gamma ray's in PET, compromises the precision of position where the radioactive decay took place and results in much lower spatial resolution in SPECT compared to PET (≈10mm vs. ≈5mm).
The main isotopes used in SPECT are 123Xe, 131I, 123I and Tc99m. Since many molecules contain iodine one can substitute the naturally occurring 127I with its radioactive counterpart isotope without changing the chemical properties of the labelled molecule.
The ideal target protein for radioligands should be a protein that exactly reflects a biological process that changes with the progression of disease, e.g., be proportional to the cell loss of DA neurons in PD. Further, the binding of the radioligand to the target protein should have multiple qualities: a high reproducibility of quantification outcomes, posses a high target to background ratio with a suitable reference region devoid of that protein, be selective to the target, be reversible allowing for displacement by unlabelled tracer, have no radiolabelled metabolites capable of crossing the BBB and finally, of course be safe and tolerable for patients and healthy volunteers.

Imaging the nigro-striatal pathway

With the introduction of PET and SPECT new insight into the neurobiology of the nigro-striatal pathway followed. The potential of PET and SPECT brain imaging provided the clinicians with new diagnostic tools [52, 53] and the pharmaceutical companies and the researchers with a biomarker for disease progression and evaluation of treatment efficacy [54, 55].

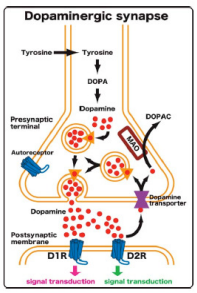

Figure 7. The conventional DA synapse. The figure illustrates various proteins that could be encountered as targets for radiotracer binding. Presynaptic: DAT, VMAT (yellow triangles) or DOPA. Postsynaptic: D1 or D2. (Source: the internet, unknown illustrator.)

The first target to be imaged in humans (by PET) was the postsynaptic receptors [56]. Of course this was especially interesting when looking at diseases with a postsynaptic pathology, e.g., as in Huntington's Disease [57]. It was also with postsynaptic radioligands that scientists were able to show endogenous release of dopamine into the synaptic cleft after stimulation [58], thereby for the first time in vivo supporting the hypothesis of hyperactivity of the DA neurotransmission in schizophrenia. Since then these receptors have been the focus of intense investigation and for example used in evaluation of antipsychotic drugs [59, 60].
Imaging disease progression in PD is different, since the pathology is primarily presynaptic. The function of the presynaptic DA neurons can be assessed with PET/SPECT in 3 ways (fig. 7) [61]: 1) L-DOPA uptake and catalyzation to dopamine ([18F]-fluorodopa), 2) VMAT ([11C]- or [18F]-dihydrotetrabenazine or 3) the DAT. [18F]-fluorodopa is a PET ligand that has been widely used in PD. It was first synthesized more than 30 years ago [62]. The accumulation of [18F] activity in striatum during [18F]-fluorodopa PET can be attributed to uptake of [18F]-fluorodopa in the presynaptic membrane, followed by its conversion to [18F]-fluorodopamine by AAAD, and uptake and trapping of [18F]-fluorodopamine into synaptic vesicles. Although reproducibility of [18F]-fluorodopa is high and within the range of DAT ligands [63] the problem with [18F]-flourodopa is its failure to accurately reflect DA synthesis: It is also taken up, metabolized and stored in other monoamine neurons in the striatum [64]) and in humans it gives rise to a radiolabeled metabolite [65]. Using [18F]-fluorodopa as a biomarker is not optimal since studies have shown that there is a compensatory upregulation of the synthesis and release of DA in PD animal models in early phases of PD [66], this initial upregulation is to be seen in contrast to the downregulation of the DAT [67-69]. This upregulation makes the timing of the PET scan in early stages of PD crucial to the interpretation of the scan results and makes interpretation of scientific data difficult.
The lack of selectivity seems also to be the problem for radioligands that bind to the VMAT. The VMATs are ATP-dependent transporters, which are nonselective and effective for both dopamine, norepinephrine and serotonin. As a consequence, imaging of VMAT in the brain provides a measurement reflecting the total number of all three neurons [70]. Studies have shown that there seems to be no initial downregulation of VMAT compared to that of the DAT [67, 71], making it less sensitive in diagnosing de novo PD patients. On the other hand VMAT is influenced to a lesser extend by L-DOPA, deprenyl, cocaine, and amphetamine [72] which could make it more useful as a biomarker for treatment efficacy.

Notably, [18F]-fluorodopa and [18F]-dihydrotetrabenazine have the same general pros and cons being PET ligands as compared to the SPECT ligands (previously addressed).

RADIOLIGANDS FOR DAT

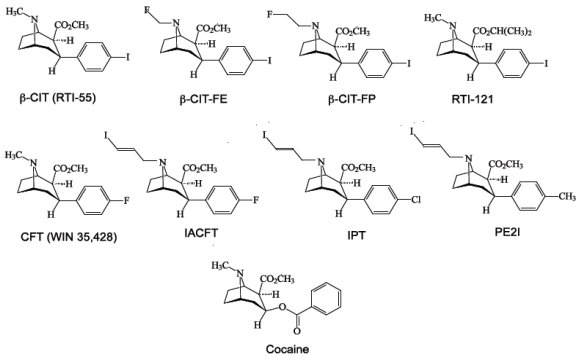

Figure 8. Radiotracers for PET/SPECT imaging.

[11C]cocaine was the first radioligand to be used for imaging the cerebral dopamine transporter in vivo [73]. A number of other radioligands have subsequently been developed and tested as PET- or SPECT ligands, however most of these ligands have been cocaine derivates (figure 8). With the introduction of 2-beta-carbomethoxy-3 beta-(4-iodophenyl)tropane ([123I]β-CIT) [74], brain imaging of DAT became a clinically useful method for supplementary diagnosis of movement disorders. As a ligand [123I]β-CIT has several serious downsides as it has equal affinity for DAT as for SERT and because of its slow kinetics it requires imaging to be conducted 24 hours after bolus injection.
A few years later 2-beta-carbomethoxy-3 beta-(4-iodophenyl)-N-(3-fluoropropyl)nortropane (FP-CIT) was synthesized [75] and its cerebral distribution and dosimetry in healthy volunteers was subsequently reported in 1998 [76]. [123I]FP-CIT has an improved selectivity for DAT vs. SERT as compared to [123I]β-CIT, se table 1.

Table 1. From (Ziebell *et al* 2010a)

SERT and DAT Binding Affinity of Inhibitor (K_i), as Measured in Rat Brain Homogenates

Ligand	K_i DAT (nM), ^{3}H-GBR-12935	K_i SERT (nM), ^{3}H-paroxetine	SERT-to-DAT ratio
^{123}I-β-CIT*	27	3	0.1
^{123}I-FP-CIT†	3.5	9.7	2.8
^{123}I-PE2I*	17	500	29.4

*According to study of Abi-Dargham et al. (5).
†According to study of Emond et al. (8).

Furthermore, due to its lower DAT affinity [123I]FP-CIT has much faster kinetic properties with a striatal peak time of 148 minutes after IV injection. As a result it has a reduced timespan of 3 hours from tracer injection to SPECT scan, making it more feasible for scanning of out hospital patients [77]. With a bolus injection and without measurements of the arterial input function, the outcome parameter (the binding ratio between a target and a reference region) does, however, become sensitive to intersubject variation in the plasma clearance rate of the radioligand [78], this will be discussed later. [123I]FP-CIT was licensed as DaTSCAN in Europe in 2000 and since then, it has become a frequently used SPECT radioligand, particularly as an ancillary tool to diagnose patients with movement disorders. In 2006 more than 500 European SPECT-centres were using [123I]FP-CIT for clinical purposes [79]. The radioligand has also been widely employed in both preclinical and clinical studies; a Pubmed search October 2010 shows that it is currently mentioned in over 300 scientific papers.
In 1997 the ligand 123-I-labelled N-(3-iodoprop-2E-enyl)-2-beta-carbomethoxy-3beta-(4-methylphenyl), named PE2I, was synthesized [80] and a dosimetry study in humans was published in 1998 [81].

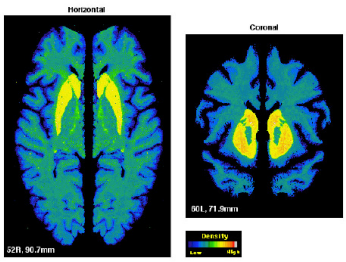

Figure 9. Distribution of DAT in the human brain using whole hemisphere autoradiography and [^{125}I]PE2I. The light green seen in the brain slice reveals a slight white matter binding (Source (Hall *et al* 1999)).

[123I]PE2I has an approximately 30-fold higher in vitro affinity for DAT than for SERT and thus in vitro results have shown that binding of [125I]PE2I is not affected by citalopram nor maprotiline [82]. The lipophilicity is high compared to that of the β-CIT (log p = 4.68, vs. log p = 4.36), and as a consequence it accumulates slightly in the white matter, fig 9. [82]. Because of its lower affinity to DAT, [123I]PE2I has faster kinetics than [123I]FP-CIT with a striatal peak time between 30-60 min [83].
PE2I has also proven suitable as a [11C] labelled PET probe [84] even also as [18F]-labelled [85], however in both circumstances the administration in humans have resulted in radiolabelled metabolites, warranting further detailed evaluations. In [123I]-labelled form neither PE2I, nor FP-CIT gave rise to radiolabelled BBB permeable metabolites [86, 87]. In spite of its favourable properties, [123I]PE2I is currently not licensed as a SPECT radioligand for clinical use.

Along with [123I]PE2I a novel 99mTc tracer was synthesised (99m)Tc-[2[[2-[[[3-(4-chlorophenyl)-8-methyl-8-azabicyclo[3,2,1]-oct-2-yl]-methyl](2-mercaptoethyl) amino]ethyl]amino]ethane-thiolato(3-)-N2,N2',S2,S2]oxo-[1R-(exo-exo) namely 99mTc-TRODAT-1 [88]. This 99mTc-based tracer has several advantages; it is less expensive than the cyclotron-produced 123I tracers and can be readily produced by a commercially available 99Mo/99mTc generator. But even though 99mTc-TRODAT-1 has a high DAT:SERT selectivity (26:1) it has the disadvantage of having a very low target to background that compromises the sensitivity of the scan [89].

QUANTIFICATION OF TARGET PROTEINS BY SPECT/PET

As previously mentioned it is important when measuring a biological system in vivo, not to interfere with the function of the system. Therefore, the labeled + unlabelled compound should not occupy more than 5-10% of the receptors, preferentially less. In most SPECT studies occupancy is less than 1 %. In vitro quantification of radiotracers bound to target proteins is based on the equilibrium binding reaction:

$R + F \leftrightarrow B$

where R is the receptor (or transporter), F is free ligand and B a complex of both.
In 1984 the binding potential was introduced for PET imaging [90] and defined as:

$$BP = \frac{B_{MAX}}{K_D}$$

where Bmax equals the receptor density and KD the radioligand equilibrium dissociation constant or the affinity of the radioligand. In the simplest form BP is a ratio of specifically bound tracer in the brain to the free concentration in the brain. This can be derived from the Michaelis–Menten equation (which is used to describe in vitro receptor binding):

$$B = \frac{B_{MAX} * F}{K_D + F}$$

$$\Rightarrow \frac{B}{F} = \frac{B_{MAX}}{K_D} = BP$$, because in radiotracer studies F<<<KD.

Since measurement of the free concentrations in the brain would require invasive procedures and thus rejecting PET and SPECT as non-invasive methods, several simplified models for measuring the BP were established. The first assumption in these models is that the free radiotracer in blood diffuses unstirred across the BBB. By this assumption one can measure the BP in a specific region of interest (ROI) in the brain as the ratio of specifically bound radioligand in the ROI to the concentration in either plasma (BPP) defined as:

$$BP_P = \frac{specifically\ bound\ radioligand}{total\ parent\ radioligand\ in\ plasma}$$

or to that of a reference region representing the concentration of non-displaceable radioligand in the brain (BPND):

$$BP_{ND} = \frac{specifically\ bound\ radioligand}{non-displaceable\ radioligand\ in\ brain\ tissue}$$

Non-displaceable radioligand equals the sum of the free and non-specific bound radioligand concentration. The specific bound radioligand is the total radioligand bound in the ROI minus the non-displaceable radioligand. Non-displaceable binding is usually represented by a region, which is assumed to be devoid of the specific receptor i.e. a reference region. By delineation of a ROI in a SPECT/PET image the mean counts of gamma-ray's can be measured as a linear function of radioligand concentration. Thus calculating the BPND without even measuring radioligand concentration in the blood:

$$BP_{ND} = \frac{C_{ROI} - C_{REFERECE}}{C_{REFERENCE}} = \frac{C_{ROI}}{C_{REFERENCE}} - 1$$

CROI = concentration in the ROI, CREFERENCE = concentration in reference region.
Yet, very importantly, the BPND is not a representation of the true BP, since several precautions are to be taken when calculating the BPND:
First of all, only a subset of receptors/transporters is available in vivo, hence the BPND does not represent the total receptor concentration but a reflection of the maximum amount available for binding (Bavail). Secondly, as the target proteins are not saturated with tracer, the BPND is directly correlated to the free fraction of the non-displaceable compartment (fND) i.e. the fraction of radioligand that is freely dissolved in tissue water in the brain, hence:

$$BP_{ND} = f_{ND} * B_{AVAILABLE} / K_D$$

Last, but not least, calculating the BPND by a concentration ratio presupposes that the concentration in plasma and brain tissue is at steady state conditions (in vivo terms of in vitro equilibrium [91]). In clinical centers this is sometimes ignored to an extent that may compromise quantification accuracy. In these cases BP is often measured when tracers appear in a steady state because of a very slow washout from the brain. However, this is a pseudo steady state condition, also termed transient equilibrium or pseudo-equlibrium. In theory, an individual binding ratio calculated at transient equilibrium could overestimate true steady state BPND if the individual terminal plasma clearance rate is high; a problem originally addressed by Carson [78].
There are several ways of calculating a true BPND and one of them is by obtaining true steady state conditions. One way this can be achieved is by a constant infusion of the radioligand, however this would be a very time consuming affair because of the continuously biologic half-life (metabolism and decay) of the radioligand. The steady state condition can therefore be hasten by the use of a bolus plus constant infusion design [78].). The idea is to hasten a true steady state of the tracer in plasma and in the brain by an initial injection of a tracer bolus prior to the tracer infusion. The ratio between the bolus and the constant infusion can be calculated from bolus injection data. The result of the calculated size of bolus relative to that of the infusion is often described as a ratio of the bolus size to the infusion velocity defined as the bolus-to-infusion ratio B/I ratio (h) [78, 92, 93]. The bolus infusion idea is illustrated in figure 10.

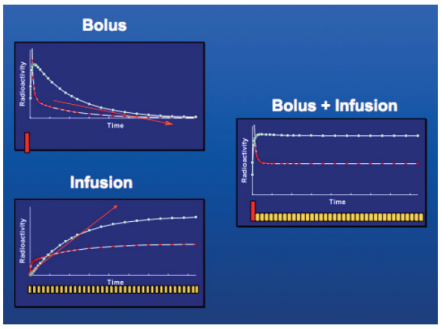

Figure 10. Light blue dots indicate time activity curves (TAC) for a brain region and red dots the plasma curve. Ideally, the infusion velocity should equal the terminal plasma clearance rate from a bolus injection, both indicated by the red arrows (Illustration kindly provided by Pinborg LH).

In addition to precise calculations of the BPND the steady state condition ease interpretation of pharmacological challenge to the target protein in the ROI, by e.g. "cold" ligand. That is, the TAC for the ROI will approach that of the reference region if the drug has affinity and thus compete with the radioligand for the target protein.
Calculating the true BPND can also be achieved using either kinetic analysis such as the Logan analysis [94] or graphical

analysis such as the Simplified Tissue Reference Model (SRTM) [95]. These analyses are attractive methods since they rely on data from bolus injection alone. The drawbacks are that the methods are more vulnerable to noise in the data and often require longer scanning time, which hinders their clinical use [96]. Finally, visual semi-quantification can also be achieved. Especially in the clinical setting this is a very popular time saving method and it is used in many centers of nuclear medicine. A visual quantification, by an experienced reader, can very often be sufficient to tell if the image is normal or abnormal. However, visual quantification cannot give any exact estimates of the receptor concentration in a ROI and is therefore useless in research perspectives. Despite of this fact a visual quantification is from time to time observed in a scientific paper [97].

AIMS

This PhD-thesis covers the investigation of the SPECT DAT radioligand [123I]PE2I which includes the following steps:

1) Establishment of a bolus/infusion (B/I) protocol for [123I]PE2I that enable steady state conditions in plasma and brain.
2) Test of reproducibility of the B/I method in healthy subjects and in patients with decreased striatal binding of [123I]PE2I.
3) Evaluation of different ROI delineation methods for [123I]PE2I quantification.
4) Comparison of binding potential and contribution of serotonin transporter binding in [123I]PE2I images as compared to the commonly used [123I]FP-CIT.

RESULTS AND DISCUSSION

The bolus infusion method for [123I]PE2I

The first aim of this study was to establish a bolus infusion method for [123I]PE2I thereby enabling easy and reliable quantification of [123I]PE2I binding to DAT in the human brain. The group had been working with [123I]PE2I for a few years before I started my research. The use of [123I]PE2I began in 1998 as part of an EU-project. With MD, DMSc Lars H. Pinborg as head of the trials the conclusion was that the non-invasive Logan analysis, a graphical analysis method provided the most accurate method for quantification [83]. This method is very accurate and does not require arterial blood samples, but the recommended study time of 120 min could be a problem in an every day clinical practice since it would compromise scanning capacity to 3 per scanner per day. In addition 2 hours spend in a scanner is not feasible for many elderly persons and Logan analysis is compromised significantly if the patient is to abort the SPECT scan. Therefore we chose to see if we could set up a bolus infusion method initially described by Carson [78], a method that the group previously had experience with [92, 93]. Five healthy volunteers were included (paper 1), and all of them were studied twice at 2 separate days. In addition, we tested the calculated B/I ratio in another independent group of 7 healthy volunteers, (paper 2).

Based on the first bolus studies we calculated the average bolus infusion ratio to be 2.5 h in the first 5 healthy volunteers (fig. 11). In order to reduce the time from bolus injection to steady state conditions we increased the ratio slightly, to 2.7 h.

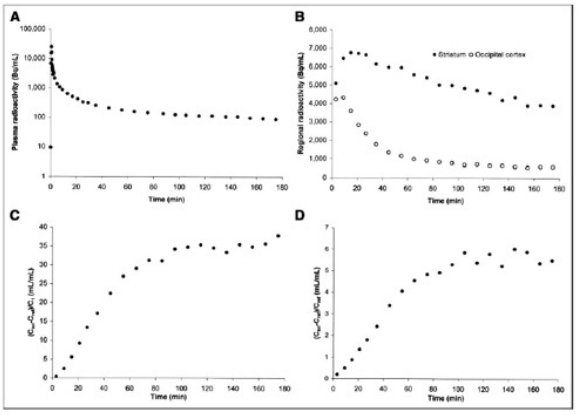

Figure 11. The results of the bolus injection studies from (Pinborg *et al* 2005). Figures 2C and 2D show the average ratio of striatum-specific binding to metabolite corrected plasma and the average ratio of striatum-specific binding to occipital cortex, respectively, as a function of time. Starting approximately 90 min after bolus injection, the curves became horizontal.

In the second scan of the 5 healthy volunteers, they received a bolus plus constant infusion and the calculated B/I ratio (2.7h) from the bolus alone study was applied. From table 2, one can appreciate the very stable BPND (at that time denoted BP2) that we achieved from 120-240 min post injection.

Table 2. From [96]

Stability of Outcome Measures, Free Parent Compound, and Individual Optimal Bolus-to-Infusion Ratio

	Bolus/infusion experiments			Bolus experiments	
Subject no.	BP_1 (%/h)	BP_2 (%/h)	Plasma (%/h)	B/I ratio (h)	Confidence interval (h)
1	−0.1	−4.0	4.2	3.7	2.4–8.5
2	6.8*	2.2	−7.2*	2.4	1.3–12.8
3	−3.1	−6.6	−2.8	3.1	2.8–3.6
4	2.8	2.1	−3.4	2.6	1.3–214.0
5	−6.6	−3.1	−4.2	1.8	1.2–4.0
Average ± SD	−0.0 ± 5.2	−1.9 ± 3.9	−1.6 ± 4.9	2.7 ± 0.7	

*Slope of regression line calculated from 120 to 240 min is significantly different from zero ($P < 0.05$). BP_1, BP_2, and plasma stability measures were calculated from bolus/infusion data. Individual bolus-to-infusion ratios and corresponding 95% confidence intervals were calculated from terminal clearance rate from plasma after bolus injection of ^{123}I-PE2I.

To get an estimate of the calculated BPND from the B/I experiments, we performed various kinetic and graphical analysis on the data from the initial bolus experiments in comparison, please see table 3. This showed that the B/I calculated BPND's did not differ significantly from the SRTM (paired students t test, P>0.3). However, as can be seen from the table, the B/I and kinetic analysis did significantly underestimate that of the transient equilibrium analysis (P< 0.0002, paired Student t test).

Table 3. From [96]

BP_2 Values Calculated Using 5 Different Methods of Quantification

		Bolus experiments			
Subject no.	Bolus/infusion experiments (120–180 min)	Reference tissue (0–180 min)	Logan analysis (0–180 min)	Peak equilibrium (40–80 min)	Transient equilibrium (90–180 min)
1	4.6	4.6	4.6	4.8	6.0
2	4.6	4.1	3.7	3.8	5.5
3	4.4	4.3	4.2	4.5	5.5
4	4.0	4.2	4.2	4.7	6.0
5	3.9	3.6	3.5	3.5	5.2
Average ± SD	4.3 ± 0.3	4.1 ± 0.4	4.0 ± 0.4	4.3 ± 0.6	5.6 ± 0.4

BP_2 was calculated using Equation 2. Peak equilibrium and transient equilibrium were not calculated at tracer steady state.

There was a very high interindividual B/I ratio and one concern about the B/I method was that it could be very difficult to calculate the individual B/I ratio. We hence did a theoretical simulation in order to calculate the maximum alterations in BPND that we could expect from wide ranges of individual terminal

plasma clearances. In the simulation we changed the B/I ratio more than 2 fold and as a result only saw a 11% variation in the calculated BPND values (figure 12).

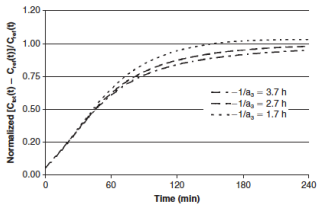

Figure 12. The average normalized BP_{ND} values are 0.99 (B/I = 1.7 h), 0.92 (B/I = 2.7 h), and 0.88 (B/I = 3.7 h). Thus, a 2.2-fold variation in terminal clearance rate from plasma translates into only a 11% variation in the calculated BP_{ND}.

So both in theory and in practice the calculated B/I ratio was quite reliable and stable and calculations of individual B/I ratios were not required. Despite of these convincing data we still wanted to test the stability in an independent sample of patients. In the next study [98] we once more tested the stability of BPND within the time window of 120-180 minutes (figure 13).

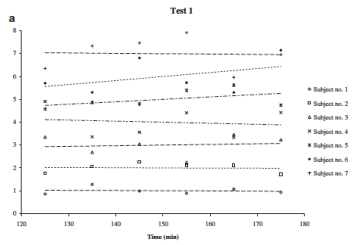

Figure 13. The stability of the BP_{ND} from the first scans of the 7 subjects (Ziebell *et al* 2007).

In table 4 the details outlines the exact values of the stability.
Table 4. From [98]

	Study 1			Study 2		
Subject	Striatum	Occipital	BP_2	Striatum	Occipital	BP_2
1	−2.5	−2.0	−5.7	2.8	1.3	2.4
2	−8.4	−7.3	−2.1	1.4	27.1	−26.8
3	−6.2	−8.8	5.3	1.8	−23.4	33.3
4	−5.1	−0.1	−7.0	−6.6	2.5	−7.7
5	−10.0	−13.9	12.6	−9.7	−21.9	14.9
6	0.4	−1.6	−4.0	3.6	5.1	−1.2
7	−7.0	−4.9	−1.5	0.1	−17.7	23.4
Mean	−5.6	−5.5	−0.3	−0.9	−3.9	5.5
SD	3.5	4.9	7.0	5.1	18.3	20.2
ABS mean	5.7	5.5	5.6	3.7	14.2	15.7

SD standard deviation, *ABS* absolute
Stability of striatal and occipital volumes: slope of time-activity curve (120–180 min)×60 min divided by mean values from 120 to 180 min in percent.
Stability of BP_2: slope of time-activity curve (estimated by striatum/occipital −1) from 120 to 180 min×60 min divided by mean values from 120 to 180 min in percent.

Even though there was a significant difference in individual BPND stability between the first and second scan of the healthy volunteers in the reproducibility study ($p < 0.03$) the overall stability was very low (≈ 5.5%). The fact that the stability measures were lower in the high count striatal ROIs than in the low count occipital cortex ROI imply that the variability was primarily due to random noise. This can be appreciated visually from figure 13 where very little change in the endpoints (120 and 180 min) can cause a large impact on the stability measurements.

REPRODUCIBILITY OF [123I]PE2I

Knowledge of the reproducibility of a method is important; not only to identify the most suitable method for quantification, but also to design studies appropriately in terms of sample size. Especially when performing costly experiments involving SPECT and PET scans an accurate power analysis is crucial to ensure that studies are not underpowered resulting in useless experiments and unnecessary exposure of radiation to healthy volunteers and/or patients. It was therefore natural to conduct reproducibility studies with radioligand [122I]PE2I. Reproducibility studies of brain SPECT imaging outcomes of DAT binding with other radioligands had already been conducted. These were carried out in both healthy volunteers [99, 100] and in patients with affected striatal DAT availability [89, 100-102] see section table.

Traditionally in DAT SPECT imaging the reproducibility is calculated as the absolute value of the difference between to measurements of BP: x1 and x2 divided by the mean given as a percentage [99].

$$\text{Reproducibility} = \frac{|x_1 - x_2|}{(x_1 + x_2)/2} * 100\%$$

This equation can be applied to the reproducibility of the total method or to different steps in the method to explore the contribution to the total reproducibility that is constituted by that particular step in the procedure. As the formula reads, one can see that the reproducibility of a given method is very much dependent of the absolute value of the observations if the difference between observation 1 and 2 remains the same. This is one of the reasons why it is important to conduct calculations of reproducibility in both healthy volunteers and in patients with a low DAT binding, since the latter according to the formula alone, should have a higher reproducibility.

In the second paper we calculated the reproducibility in 7 healthy volunteers [98] whereas we chose 8 patients with decreased striatal DAT binding in the third paper. [103].

In both studies the mean reproducibility outcomes were inversely correlated to the volume of the ROI: Ziebell et al 2007: Striatum 5.4 %, putamen 5.9 % and caudate nucleus 8.0 %; Ziebell et al 2010: Striatum11.9 %, putamen 14.8 % and caudate nucleus 19.4 % (table 5 & 6). This was probably related to delineation accuracy because of the low spatial resolution in SPECT.

Table 5. From [98]

Subject	1	2	3	4	5	6	7	Mean	SD	Reliability
Striatum BP_2										
Study 1	2.3	3.4	4.2	3.5	3.3	4.3	3.6	3.6	0.7	
Study 2	2.3	3.3	4.5	3.5	3.2	4.5	4.0	3.7	0.8	
Variability (%)	0.5	3.7	−7.0	−1.9	2.6	−3.3	−9.7	−2.2	5.4	0.96
ABS variability (%)	0.5	3.7	7.0	1.9	2.6	3.3	9.7	4.1	3.2	
Caudate nucleus BP_2										
Study 1	2.6	3.8	4.3	3.4	3.7	4.5	3.8	3.8	0.7	
Study 2	2.5	3.6	4.6	3.7	3.3	4.9	4.1	3.9	0.8	
Variability (%)	1.4	5.1	−6.4	−9.2	12.6	−6.5	−6.1	−1.3	8.0	0.95
ABS variability (%)	1.4	5.1	6.4	9.2	12.6	6.5	6.1	6.8	3.5	
Putamen BP_2										
Study 1	2.5	3.5	4.5	3.8	3.6	4.7	3.8	3.8	0.7	
Study 2	2.5	3.4	4.8	3.7	3.7	4.6	4.3	3.8	0.8	
Variability (%)	0.8	3.4	−7.1	4.2	−2.9	0.6	−11.9	−1.9	5.9	0.95
ABS variability (%)	0.8	3.4	7.1	4.2	2.9	0.6	11.9	4.4	4.0	
Striatum BP_1										
Study 1	14.5	13.9	19.9	16.3	18.8	23.8	–	18.6	4.0	
Study 2	15.4	19.9	20.3	18.9	23.0	24.9	–	21.9	3.8	
Variability (%)	−6.0	−35.7	−1.8	−14.7	−20.1	−4.8	–	−13.9	16.1	0.56
ABS variability (%)	6.0	35.7	1.8	14.7	20.1	4.8	–	13.9		
Caudate nucleus BP_1										
Study 1	16.1	15.5	19.5	18.6	19.7	25.1	–	19.1	3.4	
Study 2	17.0	21.9	21.4	21.0	24.9	25.4	–	21.9	3.0	
Variability (%)	−5.1	−34.3	−9.2	−12.3	−23.3	−1.2	–	−14.2	14.3	0.47
ABS variability (%)	5.1	34.3	9.2	12.3	23.3	1.2	–	14.2	13.2	
Putamen BP_1										
Study 1	15.6	14.3	22.0	16.4	20.2	24.8	–	18.9	4.1	
Study 2	16.5	20.6	21.1	18.4	23.8	26.7	–	21.2	3.7	
Variability (%)	−5.8	−35.9	4.2	−12.0	−16.2	−7.1	–	−12.1	13.5	0.69
ABS variability (%)	5.8	35.9	4.2	12.0	16.2	7.1	–	13.5	11.8	

ABS absolute

Table 6. From [103]

Summed Intrasubject Variability from 3 Different ROI Application Methods (n = 8)

Method	Caudate nucleus	Putamen	Striatum	ICC
MD (BP_{ND})	19.4% ± 14.3%	14.8% ± 6.0%	11.9% ± 10.0%	0.88
MRD (BP_{ND})	16.4% ± 11.9%	15.8% ± 11.7%	14.6% ± 15.3%*	0.90
SVI (SBR)			10.8% ± 10.2%	0.90

*Calculated striatum = volume-weighted (caudate nucleus + putamen).
ICC = intraclass correlation coefficient.

The final result was comparable to other available SPECT radioligands with an average reproducibility of 4.1 % and 11.9 %,

please see table 7. The section table sums up the test-retest results among SPECT DAT radioligands used in clinical practice.

Table 7. [103]

Intrasubject Variability of Various DAT Radioligands for SPECT

Study	Ligand	Total patients (*n*)	Delineation	Intrasubject variability*		Reliability ICC
				Healthy volunteers	Patients	
Ziebell et al. (*17*)	PE2I	7	MD HC	4.1 ± 3.2		0.96
Seibyl et al. (*20*)	β-CIT	7	Template WS	12.8 ± 8.9†		0.82
Booij et al. (*18*)	FP-CIT	6	Template HC	7.3 ± 3.2		0.92†
Tsuchida et al. (*21*)	FP-CIT	10	Template HC	11.1 ± 10.4		0.59
Pirker et al. (*31*)	β-CIT	9	MD HC	8.2 ± 7.2		0.70
Ziebell et al., current study	PE2I	8	MD HC		11.9 ± 10.0	0.88
Seibyl et al. (*20*)	β-CIT	7	Template WS		16.8 ± 13.3†	0.82
Booij et al. (*18*)	FP-CIT	6	Template HC		7.9 ± 6.9	0.72†
Tsuchida et al. (*21*)	FP-CIT	6	Template HC		7.8 ± 8.9	0.95
Hwang et al. (*19*)	Trodat	20	MD HC		10.2 ± 6.2	0.95

*Mean outcome for either BP_{ND} or SBR (±SD).
†Data extracted from publication.
ICC = intraclass correlation coefficient; HC = high-count slides; WS = whole striatum.

The first column shows the individual studies of DAT SPECT reproducibility, some of which originate from the late nineties. However, in spite of the development within the SPECT scanner hardware and the computer power, the procedures of reconstruction and the overall resolution have not changed within the last 14 years. The number of participants has traditionally been low; this is probably because of the large costs of a single SPECT scan compared to e.g. a blood sample. In the fourth column we listed the method used for delineation of ROI. Overall there does not seem to be any significant difference in reproducibility outcome using either manual or template based delineation. I will discuss the subject of delineation later on. The data of main interest is composed of column five, six and seven and show the reproducibility and reliability results. There is not much difference between any of the ligands. However, a difference from 4 to 13 % (seen in e.g. the healthy group) would require more subjects to be included and this difference is not negligible as we have previously shown in another test-retest study [104]. Overall the results showed what we expected, that reproducibility is higher in patients than in healthy volunteers. Important factors to take into account when designing studies (calculating power of future studies). On average [123I]PE2I had the same reproducibility as the commercially used [123I]FP-CIT. Remarkably [123I]PE2I had a higher reliability.
The reliability or the intraclass correlation coefficient (ICC) has traditionally been used in various reproducibility studies in SPECT and PET and was introduced in SPECT DAT reproducibility studies by Seibyl et al 1996. The ICC is a descriptive statistic outcome, which can be used when quantitative measurements are made on units that are organized into groups. It should be emphasized that no statistical cut off level is present when calculating the ICC. Calculation of ICC in medicine dates back 100 years [105] but the modern way of calculating ICC origins from [106]:

$$ICC = \frac{(MS_B - MS_W)}{(k-1)(MS_B + MS_W)}$$

Where MSB is the mean sum of squares between subjects, MSW the mean sum of squares within subjects and k the number of within-subject measurements. The ICC can vary between 0-1.0, but if an ICC is to take the value of ≈ 1.00 it is only possible if the MSB >>> than MSW. This is achieved if the data has a high individual variance and at the same time the reproducibility low. As noted, I recalculated the reliability from [100] which in one example was 1.00. Notably the ICC can be manipulated higher if one simply raises the absolute values e.g. by calculating binding ratios which equals BPND + 1 instead of BPND since this would decrease the MSW without affecting the MSB. This is illustrated in figure 14.

The reader should therefore always consider the absolute values of the outcome variable when interpreting results of reproducibility studies.

DELINEATION OF BRAIN REGION OF INTEREST (ROI) IN [123I]PE2I DAT IMAGING

Intrasubject variability in SPECT DAT imaging results from both biological and methodological variation. In the absence of subject-specific anatomical information (e.g. MRI), the ROI delineation is anticipated to be particularly prone to observer bias. To our knowledge this had never been formally assessed in DAT SPECT studies before and was the aim of paper 3. We did also briefly assess this in paper 2 and some of these results are also included in this section.

Overall, there are three principally different ways of delineating ROI's on the SPECT image: a) manual delineation (MD) directly on the SPECT-image; b) template guided delineation and c) delineation based on co-registration with another brain image that provides structural information, such as MRI/CT. In theory there is only limited difference between the MD and the adjustable template based delineation. The largest advantage of template based delineation compared to MD is that it is less time consuming and operator-independent [107]. An alternative to an anatomically correct ROI was described by Tossici-Bolt et al., the so-called striatal volume of interest method (SVI) [108]. This method requires no structural information on the brain of the individual patients, but involves a template of oversized ROI's, involving all striatal slices. The calculated volume of interest (VOI), the total counts within this volume, the count concentration in a reference region and a population-based estimate of the average striatal volume then forms the basis for the calculation of a striatal binding ratio (SBR) equivalent to the ratio of the specific / non-displaceable uptake. The three different methods can be visualized in figure 15.

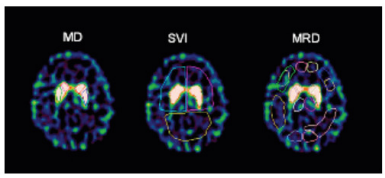

Figure 15. Three different methods of ROI delineation on SPECT images of same brain slice in same individual (Ziebell *et al* 2010b).

In healthy volunteers (paper 2) we showed that MD of ROI directly on SPECT images performed equally well to a MRI-defined probability map based ROI delineation (MRD) in terms of intrasubject variability of BPND of DAT (Manual 4.1 % vs. MRD 5.2%) [98]. This was despite the fact that the volume reproducibility of the ROI was 8 times better with the MRD method. The lack of better performance of the MRD method is probably primarily a partial volume effect related to a larger ROI volume using the MRD approach compared with the manual "hot spot" delineation approach, where ROIs are delineated on a few slices only (no attempts were made to manually move the MR-defined volumes to the "hot spots" on the SPECT image).

We expected that the test-retest variability was larger in patients with reduced DAT availability, because the concentration of tracer in the striatal regions of the patients is closer to the non-specific tracer concentrations. In this context, the method for ROI delineation without anatomical information is even more difficult and prone to larger observer bias, and the advantage of including MRI-based anatomical information for assessment of striatal DAT

availability in patients with decreased binding would be expected to have greater impact.

The ROI delineation reproducibility for each method is shown in figure 16—that is, the calculated BPND from the first ROI delineation week 0 is plotted against the BPND from the second ROI delineation 4 weeks later. The delineation reproducibility was not significantly different among any of the 3 ROI delineation methods (paired t test, P > 0.1).

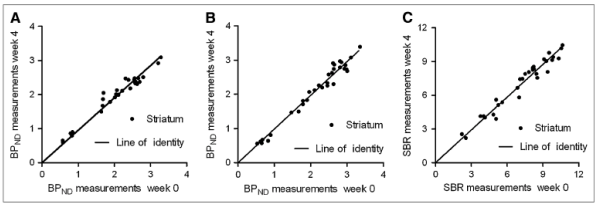

Figure 16. Intraobserver reproducibility of BPND in striatum for different delineation methods. MD (A), probability map–based delineation (B), and SVI (C). For all 3 methods, both test and retest scans were quantified entailing 32 data points (Ziebell *et al* 2010b).

Table 8 summarizes the intraobserver reproducibility of either BPND or SBR for all 3 ROI delineation methods.

Table 8. From [103].

Summed Intraobserver Reproducibility of 3 Different Methods

Method	Caudate nucleus	Putamen	Striatum	ICC
MD (BP_{ND})	10.2% ± 9.2%	9.7% ± 5.4%	7.0% ± 4.1%	0.97
MRD (BP_{ND})	14.2% ± 12.3%	8.1% ± 7.5%	5.7% ± 5.4%*	0.98
SVI (SBR)			6.7% ± 6.0%	0.98

*Calculated striatum = volume-weighted (caudate nucleus + putamen).
ICC = intraclass correlation coefficient.
No statistically significant better intraobserver reproducibility was observed for any method (MD vs. MRD, MD vs. SVI, MRD vs. SVI; $P > 0.1$), and all performed equally for intraclass correlation coefficient ($n = 16$).

Even though the results are comparable, the MD method is obviously operator dependent as well as dependent upon prior experience, and is presumably also the most time-consuming. However, the MRD method is not outperforming the other methods and especially in the every day clinical setting it is not worth the effort (since it requires an individual MRI scan in addition to the SPECT scan). The SVI method did not result in a significantly better ROI delineation reproducibility than the 2 other methods. Further, the absolute value of SBR is linearly related to the actual volume and we found a quite high interindividual variation in the MRI- determined striatal volumes, ranging from 7.2 to 10.4 mL, suggesting that the outcome parameter SBR is determined with some uncertainty if the user applies a population-based average striatal volume.
In addition to the similar ROI delineation reproducibility of the MRD compared to the MD, there was no statistically significant difference (paired t test, P > 0.4) in the BPND values calculated by the methods (Fig. 17). Linear regression analysis showed an excellent correlation with a slope of 0.99 (R2 = 0.96).

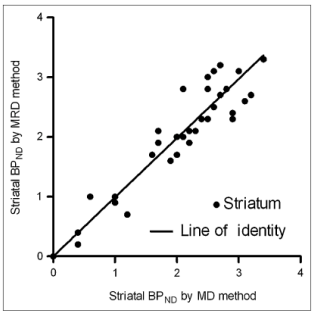

Figure 17. BP_{ND} values for caudate nucleus and putamen by ROI application with MD vs. MRD method. Linear regression analysis showed excellent correlation, $R^2 = 0.96$ (Ziebell *et al* 2010b).

The results of the reproducibility of the delineation methods should be seen in the light of the overall reproducibility of the whole method (table 9) i.e. the intrasubject variability.

Table 9. From [103].

Summed Intrasubject Variability from 3 Different ROI Application Methods ($n = 8$)

Method	Caudate nucleus	Putamen	Striatum	ICC
MD (BP_{ND})	19.4% ± 14.3%	14.8% ± 6.0%	11.9% ± 10.0%	0.88
MRD (BP_{ND})	16.4% ± 11.9%	15.8% ± 11.7%	14.6% ± 15.3%*	0.90
SVI (SBR)			10.8% ± 10.2%	0.90

*Calculated striatum = volume-weighted (caudate nucleus + putamen).
ICC = intraclass correlation coefficient.

When doing so, it is clear that the performance of the delineation reproducibility is considerable for all three methods, constituting approximately 50% of the intrasubject scan to scan variability in patients with decreased DAT binding.

HEAD TO HEAD COMPARISON OF THE DAT LIGANDS [123I]PE2I AND [123I]FP-CIT

In the fourth and final study [109] we wanted to address the in vivo selectivity of the current SPECT radioligands available for imaging of the DAT. As previously stated the in vitro selectivity for DAT compared to SERT is much higher for [123I]PE2I than for i.e. [123I]FP-CIT (10 fold, please see table 1).
However, it is well known in the radiopharmaceutical industry that in vitro selectivity and affinity is not always transferrable to in vivo settings, e.g. in vitro the β-CIT has similar affinity for DAT and SERT [74]. In contrast SPECT imaging has shown midbrain activity closely associated with DAT levels in striatum [110]. The diagram of the study is shown in figure 18.

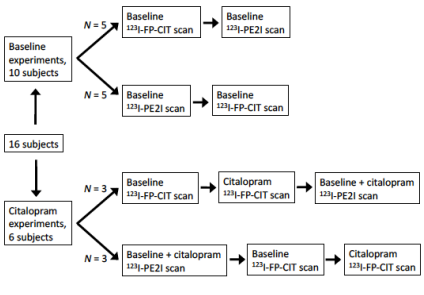

Figure 18. A total of sixteen healthy individuals were included; a diagram of the design of the study is shown in the figure (Ziebell *et al* 2010a).

Since [123I]FP-CIT is administered as a bolus alone and [123I]PE2I as a bolus followed by a constant infusion, binding parameters are not directly comparable in the baseline experiments (N=10). As the [123I]FP-CIT measurements were made 3-4 hours post bolus injection a true steady state condition was not reached whereas with [123I]PE2I, specific binding to non-displaceable binding were measured at steady state conditions. In the [123I]FP-CIT baseline experiments we therefore referred to the outcome as “binding ratios” (BR), and not BPND.

The individual striatal- and thalamic-to-cerebellum BR/BPND is shown in figure 19.

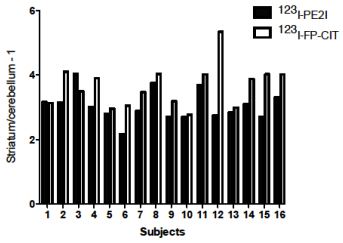

Figure 19. [123I]FP-CIT BR is significantly higher than [123I]PE2I BP_{ND} (t-test, p<0.05) (Ziebell *et al* 2010a).

Not surprisingly, the BR for [123I]FP-CIT is significantly higher than BPND for [123I]PE2I since according to our own data [96] the transient equilibrium analysis tends to overestimate the true BPND. Interestingly, we found that the actual terminal plasma clearance rate was stable with an average of ~6% decline per hour and further more, that there was no difference between BPND calculated using SRTM and the binding ratio obtained as a mean from 180-240 min post [123I]FP-CIT injection. Thus, in healthy individuals transient equilibrium analysis of [123I]FP-CIT does not explain the higher [123I]FP-CIT BR compared to BPND of [123I]PE2I. This is probably because of the slower kinetics of [123I]FP-CIT as compared to [123I]PE2I so the SRTM do underestimate the transient equilibrium analysis for [123I]FP-CIT as previously shown and discussed for [123I]PE2I [96]. As a note of caution, altered plasma clearance may occur in patients suffering from e.g. renal diseases or where the metabolism of [123I]FP-CIT is altered.

The average count rates in striatum were 3.0 ± 0.9 times higher for [123I]FP-CIT as compared to [123I]PE2I; 3.4 ± 0.9 times higher in thalamus and 2.7 ± 0.6 times higher in cerebellum. Thus, count statistics per injected MBq seem to be superior for [123I]FP-CIT compared to [123I]PE2I. This is particularly beneficial in patients with low DAT binding. The higher brain uptake of [123I]FP-CIT is beneficial and compared to [123I]PE2I it can be translated into a better determination of the target to background ratio, into a lower dose of radioactivity, or by shortening the scanning time.

To adres the in vivo SERT/DAT selectivity of [123I]PE2I and [123I]FP-CIT we first calculated the individual specific-to-nonspecific ratio in thalamus to the individual specific-to-nonspecific ratio in striatum (fig. 20). The ratio for [123I]FP-CIT was significantly higher (43%) than for [123I]PE2I (t-test, p<0.005, N=16), with a very high individual difference.

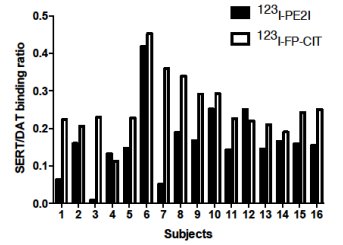

Figure 20. As a proxy for the *in vivo* SERT/DAT selectivity of [123I]PE2I and [123I]FP-CIT, the individual specific-to-nonspecific ratio in thalamus to the individual specific-to-nonspecific ratio in striatum is shown. The ratio for [123I]FP-CIT is significantly higher than for [123I]PE2I (t-test, p<0.005, N=16).

We needed to see if there could be any contribution to striatal binding of ratiotracer to SERT, therefore 6 additional healthy volunteers participated in a citalopram experiment. Citalopram was given at a dose of 0.15 mg/kg bodyweight. For [123I]FP-CIT complete TAC were obtained between 0-240 minutes so that we could fit the simplified reference tissue model (SRTM) and hence obtain true and comparable [123I]FP-CIT BPND measurements to the true steady state obtained [123I]PE2I BPND measurements. Citalopram infusion did not alter BPND for [123I]PE2I in striatum (Wilcoxon : p>0.1) figure 21.

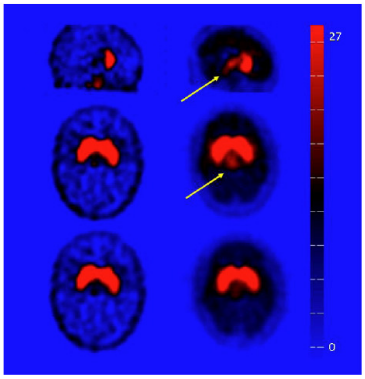

Figure 21. Example of a [123I]PE2I (left column) and [123I]FP-CIT (right column) image of the same individual. In the two first rows (sagittal and horizontal slices) the thalamus is clearly visualized in the [123I]FP-CIT image (arrows). The bottom row shows the images after acute SERT blocking with citalopram (Ziebell *et al* 2010a).

The individual BPND of [123I]FP-CIT in relation to the citalopram infusion is shown in figure 22. This illustrates how the individual striatal BPND obtained from [123I]FP-CIT approximates the BPND obtained with [123I]PE2I after citalopram infusion. After acute blocking of SERT with citalopram the 20% higher striatal specific to non-displaceable binding ratio of [123I]FP-CIT than BPND of [123I]PE2I now showed no significant difference.

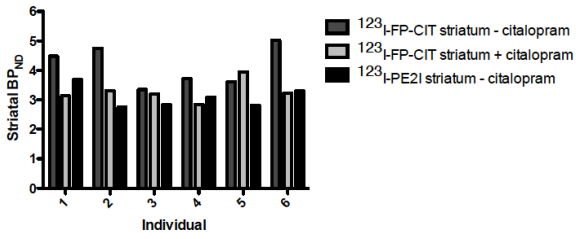

Figure 22. Demonstration of how that BP_{ND} for [123I]FP-CIT approaches the BP_{ND} for [123I]PE2I after SERT blocking by citalopram (Ziebell *et al* 2010a).

Based on the available in vitro data on [123I]FP-CIT DAT versus SERT selectivity and affinity, the extent to which SERT blocking decreased striatal BPND was larger than expected and point towards [123I]PE2I being even more selective in vivo than in vitro compared to [123I]FP-CIT.
This can be appreciated on a theoretically simulation we did (figure 23) based on the following equation:

$$\frac{SERTsignal}{TOTALsignal}\left(B_{avail,DAT}\right) = \frac{B_{avail,SERT}}{B_{avail,SERT} + \frac{K_{d,SERT}}{K_{d,DAT}} * B_{avail,DAT}}$$

SERTsignal = Bavail,SERT/Kd,SERT, TOTALsignal = Bavail,SERT/Kd,SERT + Bavail,DAT/Kd,DAT.
The binding of the radioligand to NET is neglected. Since Kd values are not available Ki are used instead and the ratio of Ki values are comparable to that of the Kd ratio.

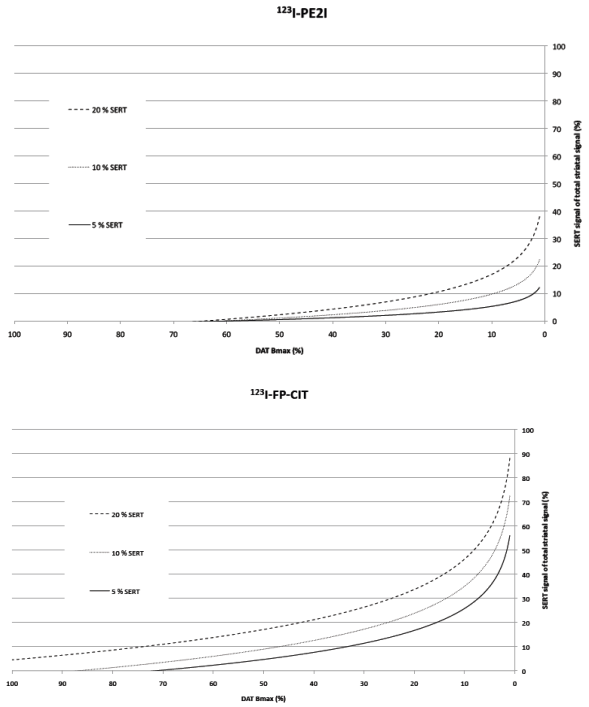

Figure 23. The figures show the theoretical proportion of SERT signal of total striatal signal in: [^{123}I]PE2I (top) and [^{123}I]FP-CIT (bottom) in a 20/1, 10/1 and 5/1 ratio of DAT/SERT distribution.

From the simulation it can be seen, that more than 20 % of the striatal transporters available should be SERT if the distribution of DAT and SERT should explain the decrease in striatal BPND we observed for [123I]FP-CIT. Human post-mortem brain studies point towards a Bavail, DAT: Bavail, SERT ratio of 20:1 in putamen ~200:10 pmol/g [7, 111]. This ratio could probably vary somewhat in healthy individuals and a large variation in BPND has indeed been reported in in vivo studies (standard deviation of BPND for SERT = 23 % of mean [112, 113]; DAT = 13% of mean [98, 100]). However, unlike [123I]PE2I binding of [123I]FP-CIT to SERT in striatum is not negligible.

CONCLUSIONS

The establishment of a B/I ratio (2.7h) for [123I]PE2I was successful. Both in theory when simulated (maximum 10% difference in BPND with 2.2 fold increase in ratio), and in clinical practice in two independent populations of healthy volunteers (BPND stability 5%/h), the B/I was confirmed to provide stable steady state measurements in plasma and in brain tissue. The B/I design is more time consuming than a simple bolus injection, but is easily implemented for routine use in a SPECT laboratory and the number of acquisitions is not compromised.

The mode of administration of [123I]FP-CIT makes it susceptible to interindividual variation in the terminal plasma clearance rate of the tracer, which may particularly be a problem in medicated patients, or patients with concomitant medical disorders. However, for healthy non-medicated individuals the influence of the terminal plasma clearance rate on the outcome parameter is not quantitatively important.

The reproducibility of the [123I]PE2I binding to DAT using the B/I is comparable to other DAT SPECT tracers with a slightly higher reliability. There was a higher reproducibility in healthy volunteers with a higher [123I]PE2I binding than in patients with low [123I]PE2I binding (≈ 3 fold) – as expected.

Anatomical precision of manual ROI delineation is compromised especially in patients with decreased striatal [123I]PE2I binding, however co-registration with structural imaging (MRI) , even with external fiducial markers, does not increase accuracy, probably because of lack in precision of co-registration. In patients with a low binding the ROI delineation constituted no matter the method a 50 % of the overall reproducibility.

[123I]PE2I showed a higher DAT/SERT in vivo selectivity than the widely and commercialized DAT radioligand [123I]FP-CIT and the results were higher than expected from in vitro measurements. Even in high binding DAT regions, binding of [123I]FP-CIT to SERT was significant and could be blocked by [123I]FP-CIT preinjection with citalopram - oppositely [123I]PE2I which was significantly unaffected. In clinical practice [123I]FP-CIT is favourable regarding count statistics per injected MBq and administration of radioligand which is less troublesome as [123I]PE2I. The easier administration of [123I]FP-CIT is usable as long as the physician that interpret the scan result keep the possible confounders (terminal plasma clearance and SSRI medication) in mind, in research perspective, however, this is more critical.

PERSPECTIVES

For the first time SPECT neuroimaging has a very in vivo selective and reliable DAT radioligand that shows high reproducibility in both patients and healthy volunteers. In addition the B/I setup provides easy interpretation of pharmacological challenges. Thus, future studies based on the data included in this thesis would be interesting. [123I]PE2I could be investigated in new studies or in replication of older studies where radioligands less DAT selective have been used. Interpretation of small differences in BP found in these studies could potentially be due to regulation in the SERT and not DAT; these are examples:

Depression in PD is common and has been the subject of research with SPECT, recently suggesting that DAT binding is lower in PD patients with depression than in PD without [114]. Based on our results, replication of such a study would be interesting to see if the extend to which the decrease in striatal [123I]FP-CIT binding is reflecting a decrease in SERT binding.

Correlation of trophic factors to the function of SPECT DAT imaging could also be potential research topics since evidence show an involvement of these factors in neurodegenerative disorders including PD [115]. Likewise the choice of a selective DAT radiotracer would be important since trophic factors also have been shown to be involved in depression [116] and hence the serotonin system.

SPECT imaging of the DAT is increasingly being used as an ancillary diagnostic tool in assessment of the diagnosis of movement disorders. The use of a selective DAT radioligand has not yet been explored. Several studies measuring the sensitivity and specificity of SPECT DAT with unselective radioligands have been carried out [117]. An unselective radioligand that is not measured at steady state conditions would tend to overestimate binding, particularly in individuals with a high SERT binding and/or high terminal plasma clearance ratio. This would give rise to a higher number of false negative DAT SPECT scan results as compared to [123I]PE2I SPECT scans. Whether this is also reflected in clinical practice remains unexplored. Within the last

couple of years the term SWEDD has evolved. This is a phenomenon covering patients with Symptoms Without Evidence of Dopaminergic Deficits. The definition alone is so far not congruent. Originally SWEDD patients were introduced in intervention studies where 10-14 % of patients although clinically well defined, surprisingly had a normal dopaminergic scan. Although most of the patients recently have been shown to have another pathology not involving striatal neurodegeneration [118], this might not be the whole truth. Of course some of them could be suffering from a non-striatal neurodegenerative disease and initially misdiagnosed, however some could have an upregulated SERT and therefore a potential abnormal [123I]PE2I scan despite of a normal [123I]FP-CIT or [123I]β-CIT scan.

SUMMARY IN ENGLISH

Imaging of the dopamine transporter (DAT) with Single Photon Emission Computer Tomography (SPECT) has increasingly been used as a biomarker for the integrity of presynaptic dopaminergic nerve cells in patients with movement disorders.
123-I-labelled N-(3-iodoprop-2E-enyl)-2-beta-carbomethoxy-3beta-(4-methylphenyl), named PE2I, has about 10-fold higher selectivity for the DAT than for the serotonin transporter (SERT) compared to the slightly older but very used and licensed radioligand [123I]FP-CIT (DaTSCAN). Further because of its lower affinity to DAT, [123I]PE2I has faster kinetics than [123I]FP-CIT with a striatal peak time between 30-60 min compared to 148 minutes for [123I]FP-CIT. Because of its fast kinetic properties, quantification of [123I]PE2I binding to DAT is possible using kinetic or graphical analysis following bolus injection of tracer or as a combination of bolus and constant infusion where constant levels in plasma and brain tissue are achieved.

A particularly important step in the DAT quantification is a correct delineation of the region of interest (ROI) in the SPECT-image. The ROI delineation can have great impact on the overall reproducibility of the method and so should be considered in reproducibility studies.

This PhD-thesis covers the investigation of the SPECT DAT radioligand [123I]PE2I which includes the following steps:

1) To establish a bolus/infusion (B/I) protocol for [123I]PE2I that enable steady state conditions in plasma and brain.
2) To test the reproducibility of the B/I method in healthy subjects and patients with decreased striatal binding of [123I]PE2I.
3) To examine different ROI delineation methods for [123I]PE2I quantification.
4) To compare binding potential and contribution of serotonin transporter binding in [123I]PE2I images as compared to [123I]FP-CIT.

Based on preliminary bolus trials we were able to calculate a B/I ratio of [123I]PE2I. This B/I ratio (2.7h) gave rise to steady state conditions and excellent reproducibility in both healthy volunteers and in patients with decreased [123I]PE2I binding. Further we showed in healthy subjects that manual delineation of ROI directly on SPECT images perform equally well to a MRI-defined probability map based ROI delineation (MRD) in terms of intrasubject variability of binding potential of DAT. In patients the expected advantage of including MRI-based anatomical information for assessment of striatal DAT availability was not present. This was probably because of difficulties in co-registration between the two image modalities even though we used external fiducials. Finally the in vivo SERT binding in DAT images obtained with [123I]FP-CIT was significant as compared to the [123I]PE2I images.

In conclusion:
Even though the only licensed radioligand for DAT imaging ([123I]FP-CIT) is selective for the DAT and easy to use, [123I]PE2I seems to be a better alternative. [123I]PE2I is a super selective SPECT DAT radioligand with optimal kinetic properties for accurate quantification of the DAT availability in striatum. Apart from the more laborious B/I design it is currently to be considered the best radioligand for imaging the DAT in the human brain with SPECT.

REFERENCES

1. Carlsson A, Lindqvist M, Magnusson T. 3,4-Dihydroxyphenylalanine and 5-hydroxytryptophan as reserpine antagonists. Nature. 1957 Nov 30;180(4596):1200.
2. Barger G, Dale HH. Chemical structure and sympathomimetic action of amines. J Physiol. 1910 Oct 11;41(1-2):19-59.
3. Holtz P. Role of L-DOPA decarboxylase in the biosynthesis of catecholamines in nervous tissue and the adrenal medulla. Pharmacol Rev. 1959 Jun;11(2, Part 2):317-29.
4. Wise RA. Dopamine, learning and motivation. Nat Rev Neurosci. 2004 Jun;5(6):483-94.
5. Falck B, Hillarp NA, Thieme G, Torp A. Fluorescence of catechol amines and related compounds condensed with formaldehyde. Brain Res Bull. 1982 Jul-Dec;9(1-6):xi-xv.
6. Anden NE, Carlsson A, Dahlstroem A, Fuxe K, Hillarp NA, Larsson K. Demonstration and Mapping out of Nigro-Neostriatal Dopamine Neurons. Life Sci. 1964 Jun;3:523-30.
7. Varnas K, Halldin C, Hall H. Autoradiographic distribution of serotonin transporters and receptor subtypes in human brain. Hum Brain Mapp. 2004 Jul;22(3):246-60.
8. Paulsen JS. Functional imaging in Huntington's disease. Exp Neurol. 2009 Apr;216(2):272-7.
9. Damier P, Hirsch EC, Agid Y, Graybiel AM. The substantia nigra of the human brain. II. Patterns of loss of dopamine-containing neurons in Parkinson's disease. Brain. 1999 Aug;122 (Pt 8):1437-48.
10. Girault JA, Greengard P. The neurobiology of dopamine signaling. Arch Neurol. 2004 May;61(5):641-4.
11. Missale C, Nash SR, Robinson SW, Jaber M, Caron MG. Dopamine receptors: from structure to function. Physiol Rev. 1998 Jan;78(1):189-225.
12. Rice ME, Cragg SJ. Dopamine spillover after quantal release: rethinking dopamine transmission in the nigrostriatal pathway. Brain Res Rev. 2008 Aug;58(2):303-13.
13. Gether U, Andersen PH, Larsson OM, Schousboe A. Neurotransmitter transporters: molecular function of important drug targets. TRENDS in Pharmacological Sciences. 2006;27(7):375-83.

14. Uhl GR. Dopamine transporter: basic science and human variation of a key molecule for dopaminergic function, locomotion, and parkinsonism. Mov Disord. 2003 Oct;18 Suppl 7:S71-80.
15. Mortensen OV, Amara SG. Dynamic regulation of the dopamine transporter. Eur J Pharmacol. 2003 Oct 31;479(1-3):159-70.
16. Piccini PP. Dopamine transporter: basic aspects and neuroimaging. Mov Disord. 2003 Oct;18 Suppl 7:S3-8.
17. Ciliax BJ, Heilman C, Demchyshyn LL, Pristupa ZB, Ince E, Hersch SM, et al. The dopamine transporter: immunochemical characterization and localization in brain. J Neurosci. 1995 Mar;15(3 Pt 1):1714-23.
18. Hersch SM, Yi H, Heilman CJ, Edwards RH, Levey AI. Subcellular localization and molecular topology of the dopamine transporter in the striatum and substantia nigra. J Comp Neurol. 1997 Nov 17;388(2):211-27.
19. Eriksen J, Rasmussen SG, Rasmussen TN, Vaegter CB, Cha JH, Zou MF, et al. Visualization of dopamine transporter trafficking in live neurons by use of fluorescent cocaine analogs. J Neurosci. 2009 May 27;29(21):6794-808.
20. Kimmel HL, Carroll FI, Kuhar MJ. Dopamine transporter synthesis and degradation rate in rat striatum and nucleus accumbens using RTI-76. Neuropharmacology. 2000 Feb 14;39(4):578-85.
21. Daws LC, Callaghan PD, Moron JA, Kahlig KM, Shippenberg TS, Javitch JA, et al. Cocaine increases dopamine uptake and cell surface expression of dopamine transporters. Biochem Biophys Res Commun. 2002 Feb 8;290(5):1545-50.
22. Letchworth SR, Nader MA, Smith HR, Friedman DP, Porrino LJ. Progression of changes in dopamine transporter binding site density as a result of cocaine self-administration in rhesus monkeys. J Neurosci. 2001 Apr 15;21(8):2799-807.
23. Eriksen J, Jorgensen TN, Gether U. Regulation of dopamine transporter function by protein-protein interactions: new discoveries and methodological challenges. J Neurochem. 2010 Apr;113(1):27-41.
24. Parkinson J. An essay on the shaking palsy. London: Sherwood, Neely, and Jones; 1817.
25. de Lau LM, Breteler MM. Epidemiology of Parkinson's disease. Lancet Neurol. 2006 Jun;5(6):525-35.
26. Katzenschlager R, Head J, Schrag A, Ben-Shlomo Y, Evans A, Lees AJ. Fourteen-year final report of the randomized PDRG-UK trial comparing three initial treatments in PD. Neurology. 2008 Aug 12;71(7):474-80.
27. Chen JJ. Parkinson's disease: health-related quality of life, economic cost, and implications of early treatment. Am J Manag Care. 2010 Mar;16 Suppl Implications:S87-93.
28. Dick FD, De Palma G, Ahmadi A, Scott NW, Prescott GJ, Bennett J, et al. Environmental risk factors for Parkinson's disease and parkinsonism: the Geoparkinson study. Occup Environ Med. 2007 Oct;64(10):666-72.
29. Lichtensteiger W, Hefti F, Felix D, Huwyler T, Melamed E, Schlumpf M. Stimulation of nigrostriatal dopamine neurones by nicotine. Neuropharmacology. 1982 Oct;21(10):963-8.
30. Solinas M, Ferre S, You ZB, Karcz-Kubicha M, Popoli P, Goldberg SR. Caffeine induces dopamine and glutamate release in the shell of the nucleus accumbens. J Neurosci. 2002 Aug 1;22(15):6321-4.
31. Evans AH, Lawrence AD, Potts J, MacGregor L, Katzenschlager R, Shaw K, et al. Relationship between impulsive sensation seeking traits, smoking, alcohol and caffeine intake, and Parkinson's disease. J Neurol Neurosurg Psychiatry. 2006 Mar;77(3):317-21.
32. Gasser T. Update on the genetics of Parkinson's disease. Mov Disord. 2007 Sep;22 Suppl 17:S343-50.
33. Pirker W, Djamshidian S, Asenbaum S, Gerschlager W, Tribl G, Hoffmann M, et al. Progression of dopaminergic degeneration in Parkinson's disease and atypical parkinsonism: a longitudinal beta-CIT SPECT study. Mov Disord. 2002 Jan;17(1):45-53.
34. van Dyck CH, Seibyl JP, Malison RT, Laruelle M, Zoghbi SS, Baldwin RM, et al. Age-related decline in dopamine transporters: analysis of striatal subregions, nonlinear effects, and hemispheric asymmetries. Am J Geriatr Psychiatry. 2002 Jan-Feb;10(1):36-43.
35. Fearnley JM, Lees AJ. Ageing and Parkinson's disease: substantia nigra regional selectivity. Brain. 1991 Oct;114 (Pt 5):2283-301.
36. Kish SJ, Tong J, Hornykiewicz O, Rajput A, Chang LJ, Guttman M, et al. Preferential loss of serotonin markers in caudate versus putamen in Parkinson's disease. Brain. 2008 Jan;131(Pt 1):120-31.
37. Strecker K, Wegner F, Hesse S, Becker GA, Patt M, Meyer PM, et al. Preserved serotonin transporter binding in de novo Parkinson's disease: negative correlation with the dopamine transporter. J Neurol. 2010 Jul 21;[Epub ahead of print].
38. Maeda T, Kannari K, Shen H, Arai A, Tomiyama M, Matsunaga M, et al. Rapid induction of serotonergic hyperinnervation in the adult rat striatum with extensive dopaminergic denervation. Neurosci Lett. 2003 May 29;343(1):17-20.
39. Eskow KL, Dupre KB, Barnum CJ, Dickinson SO, Park JY, Bishop C. The role of the dorsal raphe nucleus in the development, expression, and treatment of L-dopa-induced dyskinesia in hemiparkinsonian rats. Synapse. 2009 Jul;63(7):610-20.
40. Walker Z, Jaros E, Walker RW, Lee L, Costa DC, Livingston G, et al. Dementia with Lewy bodies: a comparison of clinical diagnosis, FP-CIT single photon emission computed tomography imaging and autopsy. J Neurol Neurosurg Psychiatry. 2007 Nov;78(11):1176-81.
41. Litvan I, MacIntyre A, Goetz CG, Wenning GK, Jellinger K, Verny M, et al. Accuracy of the clinical diagnoses of Lewy body disease, Parkinson disease, and dementia with Lewy bodies: a clinicopathologic study. Arch Neurol. 1998 Jul;55(7):969-78.
42. Hughes AJ, Daniel SE, Kilford L, Lees AJ. Accuracy of clinical diagnosis of idiopathic Parkinson's disease: a clinico-pathological study of 100 cases. J Neurol Neurosurg Psychiatry. 1992 Mar;55(3):181-4.
43. Olanow CW, Rascol O, Hauser R, Feigin PD, Jankovic J, Lang A, et al. A double-blind, delayed-start trial of rasagiline in Parkinson's disease. N Engl J Med. 2009 Sep 24;361(13):1268-78.
44. Eller M, Williams DR. Biological fluid biomarkers in neurodegenerative parkinsonism. Nat Rev Neurol. 2009 Oct;5(10):561-70.

45. Stern MB, Braffman BH, Skolnick BE, Hurtig HI, Grossman RI. Magnetic resonance imaging in Parkinson's disease and parkinsonian syndromes. Neurology. 1989 Nov;39(11):1524-6.
46. Minati L, Grisoli M, Carella F, De Simone T, Bruzzone MG, Savoiardo M. Imaging degeneration of the substantia nigra in Parkinson disease with inversion-recovery MR imaging. AJNR Am J Neuroradiol. 2007 Feb;28(2):309-13.
47. Michaeli S, Oz G, Sorce DJ, Garwood M, Ugurbil K, Majestic S, et al. Assessment of brain iron and neuronal integrity in patients with Parkinson's disease using novel MRI contrasts. Mov Disord. 2007 Feb 15;22(3):334-40.
48. Geng DY, Li YX, Zee CS. Magnetic resonance imaging-based volumetric analysis of basal ganglia nuclei and substantia nigra in patients with Parkinson's disease. Neurosurgery. 2006 Feb;58(2):256-62; discussion -62.
49. Vaillancourt DE, Spraker MB, Prodoehl J, Abraham I, Corcos DM, Zhou XJ, et al. High-resolution diffusion tensor imaging in the substantia nigra of de novo Parkinson disease. Neurology. 2009 Apr 21;72(16):1378-84.
50. Kuhl D, Edwards R. Image separation radioisotope scanning. Radiology. 1963;80:653-61.
51. Lassen NA, Henriksen L, Paulson OB. Regional cerebral blood flow by radioxenon-113 inhalation and dynamic emission tomography. Prog Nucl Med. 1981;7:110-7.
52. Catafau AM, Tolosa E. Impact of dopamine transporter SPECT using 123I-Ioflupane on diagnosis and management of patients with clinically uncertain Parkinsonian syndromes. Mov Disord. 2004 Oct;19(10):1175-82.
53. Vlaar AM, de Nijs T, Kessels AG, Vreeling FW, Winogrodzka A, Mess WH, et al. Diagnostic value of 123I-ioflupane and 123I-iodobenzamide SPECT scans in 248 patients with parkinsonian syndromes. Eur Neurol. 2008;59(5):258-66.
54. Dopamine transporter brain imaging to assess the effects of pramipexole vs levodopa on Parkinson disease progression. JAMA. 2002 Apr 3;287(13):1653-61.
55. Fahn S, Oakes D, Shoulson I, Kieburtz K, Rudolph A, Lang A, et al. Levodopa and the progression of Parkinson's disease. N Engl J Med. 2004 Dec 9;351(24):2498-508.
56. Wagner HN, Jr., Burns HD, Dannals RF, Wong DF, Langstrom B, Duelfer T, et al. Imaging dopamine receptors in the human brain by positron tomography. Science. 1983 Sep 23;221(4617):1264-6.
57. Pinborg LH, Videbaek C, Hasselbalch SG, Sorensen SA, Wagner A, Paulson OB, et al. Benzodiazepine receptor quantification in Huntington's disease with [(123)I]omazenil and SPECT. J Neurol Neurosurg Psychiatry. 2001 May;70(5):657-61.
58. Laruelle M, Abi-Dargham A, van Dyck CH, Gil R, D'Souza CD, Erdos J, et al. Single photon emission computerized tomography imaging of amphetamine-induced dopamine release in drug-free schizophrenic subjects. Proc Natl Acad Sci U S A. 1996 Aug 20;93(17):9235-40.
59. Catafau AM, Corripio I, Perez V, Martin JC, Schotte A, Carrio I, et al. Dopamine D2 receptor occupancy by risperidone: implications for the timing and magnitude of clinical response. Psychiatry Res. 2006 Dec 1;148(2-3):175-83.
60. Corripio I, Catafau AM, Perez V, Puigdemont D, Mena E, Aguilar Y, et al. Striatal dopaminergic D2 receptor occupancy and clinical efficacy in psychosis exacerbation: a 123I-IBZM study with ziprasidone and haloperidol. Prog Neuropsychopharmacol Biol Psychiatry. 2005 Jan;29(1):91-6.
61. Brooks DJ, Frey KA, Marek KL, Oakes D, Paty D, Prentice R, et al. Assessment of neuroimaging techniques as biomarkers of the progression of Parkinson's disease. Exp Neurol. 2003 Nov;184 Suppl 1:S68-79.
62. Garnett ES, Firnau G, Chan PK, Sood S, Belbeck LW. [18F]fluoro-dopa, an analogue of dopa, and its use in direct external measurements of storage, degradation, and turnover of intracerebral dopamine. Proc Natl Acad Sci U S A. 1978 Jan;75(1):464-7.
63. Vingerhoets FJ, Schulzer M, Ruth TJ, Holden JE, Snow BJ. Reproducibility and discriminating ability of fluorine-18-6-fluoro-L-Dopa PET in Parkinson's disease. J Nucl Med. 1996 Mar;37(3):421-6.
64. Brown WD, Taylor MD, Roberts AD, Oakes TR, Schueller MJ, Holden JE, et al. FluoroDOPA PET shows the nondopaminergic as well as dopaminergic destinations of levodopa. Neurology. 1999 Oct 12;53(6):1212-8.
65. Luxen A, Guillaume M, Melega WP, Pike VW, Solin O, Wagner R. Production of 6-[18F]fluoro-L-dopa and its metabolism in vivo--a critical review. Int J Rad Appl Instrum B. 1992 Feb;19(2):149-58.
66. Zigmond MJ, Abercrombie ED, Berger TW, Grace AA, Stricker EM. Compensations after lesions of central dopaminergic neurons: some clinical and basic implications. Trends Neurosci. 1990 Jul;13(7):290-6.
67. Lee CS, Samii A, Sossi V, Ruth TJ, Schulzer M, Holden JE, et al. In vivo positron emission tomographic evidence for compensatory changes in presynaptic dopaminergic nerve terminals in Parkinson's disease. Ann Neurol. 2000 Apr;47(4):493-503.
68. Tedroff J, Ekesbo A, Rydin E, Langstrom B, Hagberg G. Regulation of dopaminergic activity in early Parkinson's disease. Ann Neurol. 1999 Sep;46(3):359-65.
69. Fernandez HH, Friedman JH, Fischman AJ, Noto RB, Lannon MC. Is altropane SPECT more sensitive to fluoroDOPA PET for detecting early Parkinson's disease? Med Sci Monit. 2001 Nov-Dec;7(6):1339-43.
70. Frey KA, Koeppe RA, Kilbourn MR. Imaging the vesicular monoamine transporter. Adv Neurol. 2001;86:237-47.
71. Kilbourn MR, Kuszpit K, Sherman P. Rapid and differential losses of in vivo dopamine transporter (DAT) and vesicular monoamine transporter (VMAT2) radioligand binding in MPTP-treated mice. Synapse. 2000 Mar 15;35(4):250-5.
72. Wilson JM, Kish SJ. The vesicular monoamine transporter, in contrast to the dopamine transporter, is not altered by chronic cocaine self-administration in the rat. J Neurosci. 1996 May 15;16(10):3507-10.
73. Fowler JS, Volkow ND, Wolf AP, Dewey SL, Schlyer DJ, Macgregor RR, et al. Mapping cocaine binding sites in human and baboon brain in vivo. Synapse. 1989;4(4):371-7.
74. Neumeyer JL, Wang SY, Milius RA, Baldwin RM, Zea-Ponce Y, Hoffer PB, et al. [123I]-2 beta-carbomethoxy-3 beta-(4-iodophenyl)tropane: high-affinity SPECT radiotracer of monoamine reuptake sites in brain. J Med Chem. 1991 Oct;34(10):3144-6.

75. Neumeyer JL, Wang S, Gao Y, Milius RA, Kula NS, Campbell A, et al. N-omega-fluoroalkyl analogs of (1R)-2 beta-carbomethoxy-3 beta-(4-iodophenyl)-tropane (beta-CIT): radiotracers for positron emission tomography and single photon emission computed tomography imaging of dopamine transporters. J Med Chem. 1994 May 27;37(11):1558-61.
76. Booij J, Busemann Sokole E, Stabin MG, Janssen AG, de Bruin K, van Royen EA. Human biodistribution and dosimetry of [123I]FP-CIT: a potent radioligand for imaging of dopamine transporters. Eur J Nucl Med. 1998 Jan;25(1):24-30.
77. Abi-Dargham A, Gandelman MS, DeErausquin GA, Zea-Ponce Y, Zoghbi SS, Baldwin RM, et al. SPECT imaging of dopamine transporters in human brain with iodine-123-fluoroalkyl analogs of beta-CIT. J Nucl Med. 1996 Jul;37(7):1129-33.
78. Carson RE, Channing MA, Blasberg RG, Dunn BB, Cohen RM, Rice KC, et al. Comparison of bolus and infusion methods for receptor quantitation: application to [18F]cyclofoxy and positron emission tomography. J Cereb Blood Flow Metab. 1993 Jan;13(1):24-42.
79. Booij J, Kemp P. Dopamine transporter imaging with [(123)I]FP-CIT SPECT: potential effects of drugs. Eur J Nucl Med Mol Imaging. 2008 Feb;35(2):424-38.
80. Emond P, Garreau L, Chalon S, Boazi M, Caillet M, Bricard J, et al. Synthesis and ligand binding of nortropane derivatives: N-substituted 2beta-carbomethoxy-3beta-(4'-iodophenyl)nortropane and N-(3-iodoprop-(2E)-enyl)-2beta-carbomethoxy-3beta-(3',4'-disubstituted phenyl)nortropane. New high-affinity and selective compounds for the dopamine transporter. J Med Chem. 1997 Apr 25;40(9):1366-72.
81. Kuikka JT, Baulieu JL, Hiltunen J, Halldin C, Bergstrom KA, Farde L, et al. Pharmacokinetics and dosimetry of iodine-123 labelled PE2I in humans, a radioligand for dopamine transporter imaging. Eur J Nucl Med. 1998 May;25(5):531-4.
82. Hall H, Halldin C, Guilloteau D, Chalon S, Emond P, Besnard J, et al. Visualization of the dopamine transporter in the human brain postmortem with the new selective ligand [125I]PE2I. Neuroimage. 1999 Jan;9(1):108-16.
83. Pinborg LH, Videbaek C, Svarer C, Yndgaard S, Paulson OB, Knudsen GM. Quantification of [(123)I]PE2I binding to dopamine transporters with SPET. Eur J Nucl Med Mol Imaging. 2002 May;29(5):623-31.
84. Delorenzo C, Kumar JD, Zanderigo F, Mann JJ, Parsey RV. Modeling considerations for in vivo quantification of the dopamine transporter using [(11)C]PE2I and positron emission tomography. J Cereb Blood Flow Metab. 2009 May 20;29:1332-45.
85. Schou M, Steiger C, Varrone A, Guilloteau D, Halldin C. Synthesis, radiolabeling and preliminary in vivo evaluation of [18F]FE-PE2I, a new probe for the dopamine transporter. Bioorg Med Chem Lett. 2009 Aug 15;19(16):4843-5.
86. Seibyl JP, Marek K, Sheff K, Zoghbi S, Baldwin RM, Charney DS, et al. Iodine-123-beta-CIT and iodine-123-FPCIT SPECT measurement of dopamine transporters in healthy subjects and Parkinson's patients. J Nucl Med. 1998 Sep;39(9):1500-8.
87. Videbaek C, G.M. K, K. B. Octanol extraction yields similar results as HPLC for quantitation of [123I]PE2I metabolism. Eur J Nucl Med. 1999;26:1139.
88. Kung MP, Stevenson DA, Plossl K, Meegalla SK, Beckwith A, Essman WD, et al. [99mTc]TRODAT-1: a novel technetium-99m complex as a dopamine transporter imaging agent. Eur J Nucl Med. 1997 Apr;24(4):372-80.
89. Hwang WJ, Yao WJ, Wey SP, Ting G. Reproducibility of 99mTc-TRODAT-1 SPECT measurement of dopamine transporters in Parkinson's disease. J Nucl Med. 2004 Feb;45(2):207-13.
90. Mintun MA, Raichle ME, Kilbourn MR, Wooten GF, Welch MJ. A quantitative model for the in vivo assessment of drug binding sites with positron emission tomography. Ann Neurol. 1984 Mar;15(3):217-27.
91. Innis RB, Cunningham VJ, Delforge J, Fujita M, Gjedde A, Gunn RN, et al. Consensus nomenclature for in vivo imaging of reversibly binding radioligands. J Cereb Blood Flow Metab. 2007 Sep;27(9):1533-9.
92. Pinborg LH, Adams KH, Svarer C, Holm S, Hasselbalch SG, Haugbol S, et al. Quantification of 5-HT2A receptors in the human brain using [18F]altanserin-PET and the bolus/infusion approach. J Cereb Blood Flow Metab. 2003 Aug;23(8):985-96.
93. Pinborg LH, Videbaek C, Knudsen GM, Swahn CG, Halldin C, Friberg L, et al. Dopamine D(2) receptor quantification in extrastriatal brain regions using [(123)I]epidepride with bolus/infusion. Synapse. 2000 Jun 15;36(4):322-9.
94. Logan J, Fowler JS, Volkow ND, Wolf AP, Dewey SL, Schlyer DJ, et al. Graphical analysis of reversible radioligand binding from time-activity measurements applied to [N-11C-methyl]-(-)-cocaine PET studies in human subjects. J Cereb Blood Flow Metab. 1990 Sep;10(5):740-7.
95. Lammertsma AA, Hume SP. Simplified reference tissue model for PET receptor studies. Neuroimage. 1996 Dec;4(3 Pt 1):153-8.
96. Pinborg LH, Ziebell M, Frokjaer VG, de Nijs R, Svarer C, Haugbol S, et al. Quantification of 123I-PE2I binding to dopamine transporter with SPECT after bolus and bolus/infusion. J Nucl Med. 2005 Jul;46(7):1119-27.
97. McKeith I, O'Brien J, Walker Z, Tatsch K, Booij J, Darcourt J, et al. Sensitivity and specificity of dopamine transporter imaging with 123I-FP-CIT SPECT in dementia with Lewy bodies: a phase III, multicentre study. Lancet Neurol. 2007 Apr;6(4):305-13.
98. Ziebell M, Thomsen G, Knudsen GM, de Nijs R, Svarer C, Wagner A, et al. Reproducibility of [123I]PE2I binding to dopamine transporters with SPECT. Eur J Nucl Med Mol Imaging. 2007 Jan;34(1):101-9.
99. Seibyl JP, Laruelle M, van Dyck CH, Wallace E, Baldwin RM, Zoghbi S, et al. Reproducibility of iodine-123-beta-CIT SPECT brain measurement of dopamine transporters. J Nucl Med. 1996 Feb;37(2):222-8.
100. Booij J, Habraken JB, Bergmans P, Tissingh G, Winogrodzka A, Wolters EC, et al. Imaging of dopamine transporters with iodine-123-FP-CIT SPECT in healthy controls and patients with Parkinson's disease. J Nucl Med. 1998 Nov;39(11):1879-84.
101. Seibyl JP, Marek K, Sheff K, Baldwin RM, Zoghbi S, Zea-Ponce Y, et al. Test/retest reproducibility of iodine-123-betaCIT SPECT brain measurement of dopamine

transporters in Parkinson's patients. J Nucl Med. 1997 Sep;38(9):1453-9.
102. Tsuchida T, Ballinger JR, Vines D, Kim YJ, Utsunomiya K, Lang AE, et al. Reproducibility of dopamine transporter density measured with 123I-FPCIT SPECT in normal control and Parkinson's disease patients. Ann Nucl Med. 2004 Oct;18(7):609-16.
103. Ziebell M, Pinborg LH, Thomsen G, de Nijs R, Svarer C, Wagner A, et al. MRI-guided region-of-interest delineation is comparable to manual delineation in dopamine transporter SPECT quantification in patients: a reproducibility study. J Nucl Med Technol. 2010 Jun;38(2):61-8.
104. Haugbol S, Pinborg LH, Arfan HM, Frokjaer VM, Madsen J, Dyrby TB, et al. Reproducibility of 5-HT2A receptor measurements and sample size estimations with [18F]altanserin PET using a bolus/infusion approach. Eur J Nucl Med Mol Imaging. 2007 Jun;34(6):910-5.
105. Arthur Harris J. On the Calculation of Intra-Class and Inter-Class Coefficients of Correlation from Class Moments when the Number of Possible Combinations is Large. Biometrika. 1913;9(3/4):446-72.
106. Kirk R. Experimental design: procedures for the behavioral sciences. Pacific Grove, CA: Brooks/Cole; 1982.
107. Koch W, Radau PE, Hamann C, Tatsch K. Clinical testing of an optimized software solution for an automated, observer-independent evaluation of dopamine transporter SPECT studies. J Nucl Med. 2005 Jul;46(7):1109-18.
108. Tossici-Bolt L, Hoffmann SM, Kemp PM, Mehta RL, Fleming JS. Quantification of [(123)I]FP-CIT SPECT brain images: an accurate technique for measurement of the specific binding ratio. Eur J Nucl Med Mol Imaging. 2006 Dec;33(12):1491-9.
109. Ziebell M, Holm-Hansen S, Thomsen G, Wagner A, Jensen P, Pinborg LH, et al. Serotonin transporters in dopamine transporter imaging: A head-to-head comparison of dopamine transporter SPECT radioligands [123I]FP-CIT and [123I]PE2I. J Nucl Med. 2010;Accepted Sep 2010.
110. Laruelle M, Baldwin RM, Malison RT, Zea-Ponce Y, Zoghbi SS, al-Tikriti MS, et al. SPECT imaging of dopamine and serotonin transporters with [123I]beta-CIT: pharmacological characterization of brain uptake in nonhuman primates. Synapse. 1993 Apr;13(4):295-309.
111. Madras BK, Gracz LM, Fahey MA, Elmaleh D, Meltzer PC, Liang AY, et al. Altropane, a SPECT or PET imaging probe for dopamine neurons: III. Human dopamine transporter in postmortem normal and Parkinson's diseased brain. Synapse. 1998 Jun;29(2):116-27.
112. Matsumoto R, Ichise M, Ito H, Ando T, Takahashi H, Ikoma Y, et al. Reduced serotonin transporter binding in the insular cortex in patients with obsessive-compulsive disorder: A [(11)C]DASB PET study. Neuroimage. 2009 Aug 4;49:121-6.
113. Frankle WG, Slifstein M, Gunn RN, Huang Y, Hwang DR, Darr EA, et al. Estimation of serotonin transporter parameters with 11C-DASB in healthy humans: reproducibility and comparison of methods. J Nucl Med. 2006 May;47(5):815-26.
114. Hesse S, Meyer PM, Strecker K, Barthel H, Wegner F, Oehlwein C, et al. Monoamine transporter availability in Parkinson's disease patients with or without depression. Eur J Nucl Med Mol Imaging. 2009 Mar;36(3):428-35.
115. Zuccato C, Cattaneo E. Brain-derived neurotrophic factor in neurodegenerative diseases. Nat Rev Neurol. 2009 Jun;5(6):311-22.
116. Brunoni AR, Lopes M, Fregni F. A systematic review and meta-analysis of clinical studies on major depression and BDNF levels: implications for the role of neuroplasticity in depression. Int J Neuropsychopharmacol. 2008 Dec;11(8):1169-80.
117. Vlaar AM, van Kroonenburgh MJ, Kessels AG, Weber WE. Meta-analysis of the literature on diagnostic accuracy of SPECT in parkinsonian syndromes. BMC Neurol. 2007;7:27.
118. Marshall VL, Reininger CB, Marquardt M, Patterson J, Hadley DM, Oertel WH, et al. Parkinson's disease is overdiagnosed clinically at baseline in diagnostically uncertain cases: a 3-year European multicenter study with repeat [123I]FP-CIT SPECT. Mov Disord. 2009 Mar 15;24(4):500-8.